UNIVERSITY OF THESSALY

SCHOOL OF ENGINEERING
DEPARTMENT OF MECHANICAL ENGINEERING

Numerical Calculation of Stress Concentration Factors in Shafts with U-Shaped Circumferential Grooves and Comparison with Theoretical Results

By

Angelinas Konstantinos (AM 1565)

A thesis submitted in partial fulfillment of the requirements for the degree of Diploma

in Mechanical Engineering at the University of Thessaly

Volos, 2023

Approved by the committee of final examination:

Advisor	Dr. Sotiria Chouliara, Lab Teaching Personnel, Department of Mechanical Engineering, University of Thessaly
Member	Dr. Nikolaos Aravas, Professor, Department of Mechanical Engineering, Aristotle University of Thessaly
Member	Dr. Alexis Kermanidis, Associate Professor, Department of Mechanical Engineering, University of Thessaly

Date Approved: 28/02/2023

Acknowledgements

Foremost, I would like to express my sincere gratitude to my thesis supervisor Dr. Sotiria Chouliara for the continuous support of my graduate study and research, her guidance and patience with me. Her encouragement during my research and her willingness to help me with the research problems that I confronted, has shown me how to work with integrity. From the beginning of the research to the completion Dr. Chouliara has guided me and assisted me in appreciation of this topic.

Besides my advisor, I would also like to thank my professors, Dr. Nikolaos Aravas and Dr. Alexis Kermanidis, for willing to participate in the final examination committee and for the knowledge they gave me during my studies in the Department of Mechanical Engineering at University of Thessaly.

I am also sincerely thankful to my parents for their encouragement, guidance and financial support throughout my studies. Without them, I would not be able to pursue my goals and dreams. Last but no least, I would like to thank my friends and my girlfriend Anna, who supported me mentally, encouraged me and also proffered many consultation that were helpful during my thesis work.

Numerical Calculation of Stress Concentration Factors in Shafts with U-Shaped Circumferential Grooves and Comparison with Theoretical Results

Angelinas Konstantinos

Department of Mechanical Engineering, University of Thessaly

Supervisor: Dr. Sotiria Chouliara

Lab Teaching Personnel

Abstract

Dimensional changes and discontinuities of a member in a loaded structure, such as shoulders, grooves, holes, keyways, threads or cracks, will lead to variations of stress and much larger magnitudes of stresses than the average stress over the whole section, near these discontinuities. Most of the mechanical structures and components have such weak points, and as a result, stress concentration in structural members is a classic topic of mechanical engineering and it is strongly associated with machine elements such as shafts.

The purpose of this diploma thesis is the numerical study and calculation of stress concentration due to geometric discontinuities. This numerical study especially focuses in shafts with U-Shaped circumferential grooves under tension and is accomplished with the help of Finite Elements methods (via Abaqus), in order to determine the corresponding stress concentration factors (SCF, Kt) considering various parameters. Then, the numerical results are compared with theoretical results available by previous studies.

Contents

Chapter 1

1.1. Introduction

In theoretical materials science, it is commonly assumed that there aren't any abnormalities in the material of the specimen under tension, torsion or bending, neither any discontinuity on it, in order to determine the developing stresses. In reality, things are a lot different.

In this first chapter of the study, we will make an introduction to the stress analysis of shafts. As in this diploma thesis we mainly study the effect of stress concentration on a shaft with U-Shaped circumferential grooves under tension, we will first study the effect of the geometry of the shaft on the stress concentration phenomenon, in general.

By the term shaft, we usually refer to a relatively long member of round cross section that rotates and transmits power. Other members such as gears, pulleys, cams, etc. are attached to the shaft by means of pins, keys, splines, snap rings and other devices. These members serve to connect the shaft to its source of power or load.

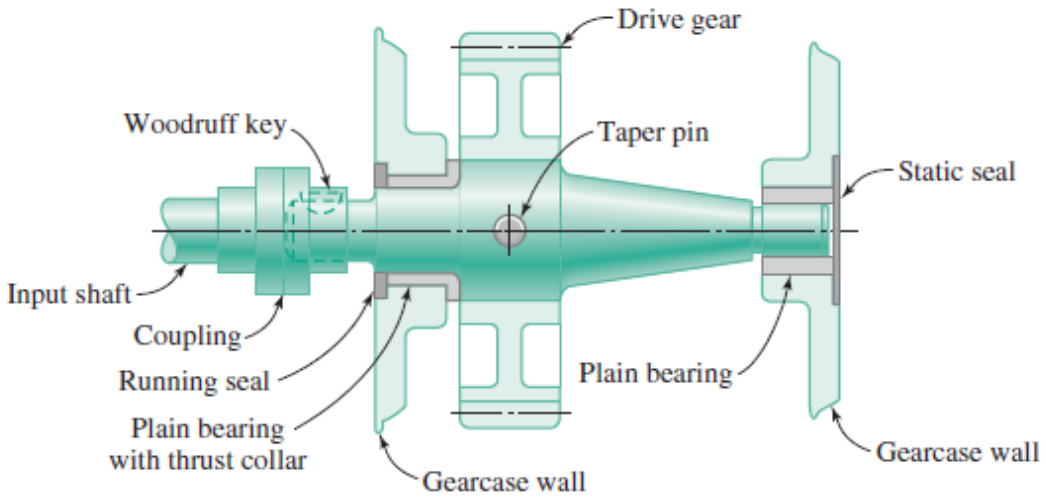

Figure 1 Sketch of a typical gear support shaft [1]

A shaft can also have a nonround cross section and it doesn't need to rotate. It can be stationary and serve to support a rotating member, such as the short shafts that support the nondriving wheels of an automobile. The shafts supporting idler gears can be either rotating or stationary, depending on whether the gear is attached to the shaft or supported by it through bearings. Shafts supporting and driving vehicle wheels are also called axles.

Shafts and axles that are used as mechanical compartments of more compound constructions, are not usually commercially available in the form that want, in order to fulfill their purpose. Of course we can find perfectly cylindrical solid or hollow shafts in standard diameters that need to be processed in order to be used. Shafts and axles can be machined, on lathes or drilling

machines, so that they come into the right shape. Therefore they may not be uniform in their entire length. On the contrary, they can obtain gradation in their diameter, form wedges for the placement of sprockets, flywheels, cranks, pulleys and gears, or even cut gears or cams on them and form a single component, and this serves their main purpose, which is to transmit power or motion.

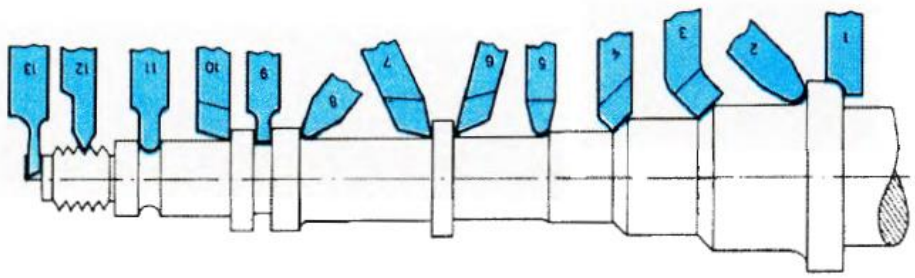

Figure 2 A stepped shaft after machining on a standard diameter commercially available cylindrical shaft. [2]

As a result, dimensional changes and discontinuity of them, lead to variations of stress, so high stresses concentrate near these dimensional changes and stress distribution is not uniform throughout the cross section, leading to stress concentration regions, at which failure can occur.

This situation of stresses near dimensional changes and discontinuities such as holes, sharp corners, cracks, etc. is called stress concentration (SC) and the ratio of peak stress near stress raiser to an average stress over the member, is called stress concentration factor (SCF). When calculating the shafts in dynamic but also in static loading, this parameter is particularly important and must be considered. We will study Stress Concentration and Stress Concentration Factor, in more detail, in the next chapter.

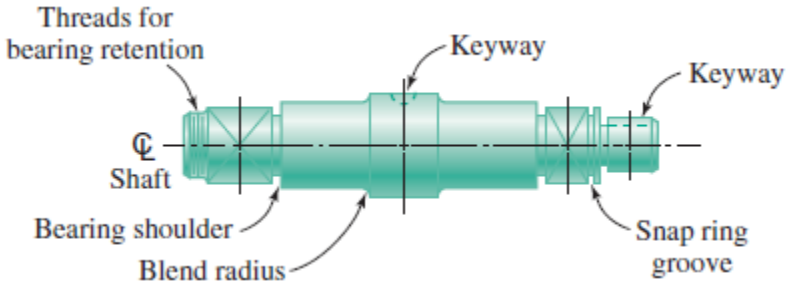

Figure 3 Shaft with shoulders, fillets and retention features [1]

Theoretical and experimental research about the influence of notches of all kind on the stress concentration has not yet been completed, as the strain of the shafts corresponds to a complex load and is very difficult to be determined. Although, the hitherto known results of this research have led to the formation of a clear picture of the stresses developing in the area of the notch.

There are practically three categories of methods used in order to perform a stress analysis on a specimen and calculate the SCF, and these are the following:

i) Experimental methods

There are many cases in which the SCF for different kinds of notches has been determined with experimental methods, but the results are only valid for the elastic area of materials. The most common experimental method, among others is the photoelasticity stress analysis. This method utilizes a birefringent model of the actual structure to view the stress contours due to external loading or residual birefringence. When white light is used for illumination, a colourful fringe pattern reveals the stress/strain distribution in the part. Using monochromatic light enable better definition of fringes especially in areas with dense fringes as at stress concentration points. [3]

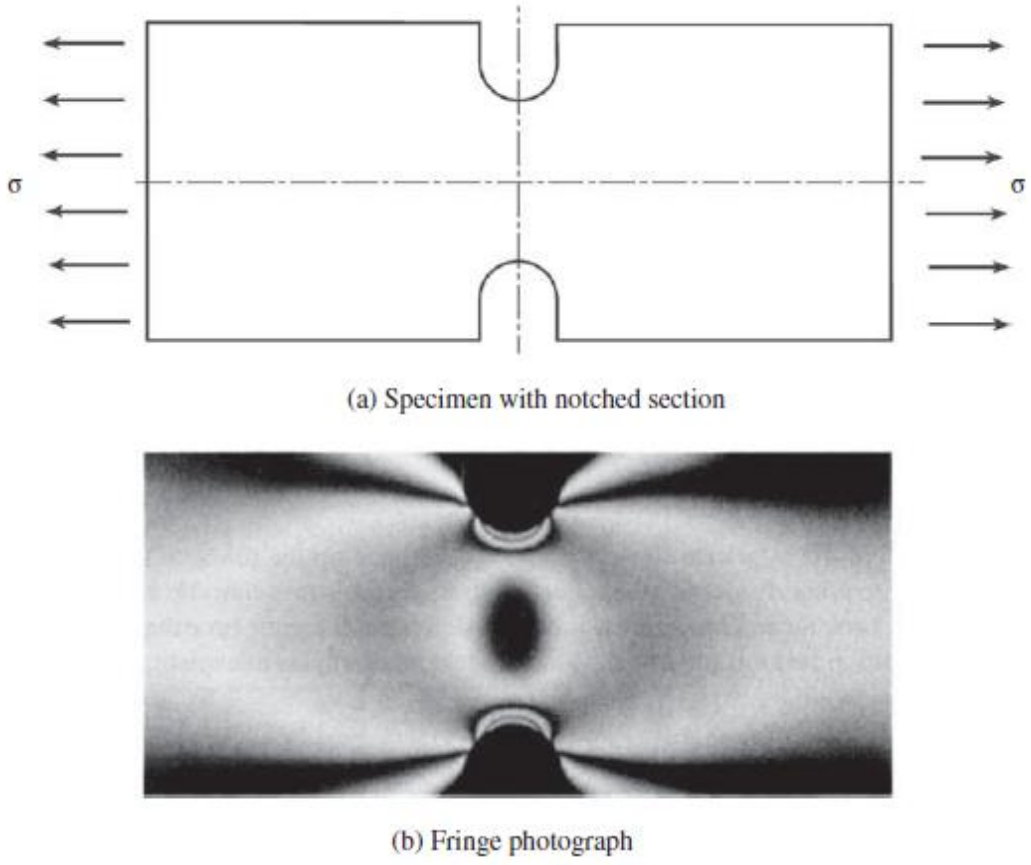

Figure 4 Stress Concentration of tension bar by notches (Doz Dr-ing habil K. Fethke, Universitat Rostock) [4]

Another experimental method for the determination of the SCF is with the use of extensometers. Extensometers, also called strain transducers or strain sensors, are measuring devices used in materials testing to measure the change in length or width, directly on the specimen. The strain is determined on the basis of the deformation of the material. As technology is developing, modern extensometers can provide very accurate results and accurate approximations of the SCF.

ii) Analytical methods

Theoretical calculation results for the stress distribution can also be gained by the solutions of equations available in literature. Although experimental methods give the most reliable results as a procedure, it is very costly and it requires special equipment, testing facilities, etc. The first mathematical study on stress concentration was published in the first decade of 20^{th} century and studies are published until today for different geometries, considering different parameters such as the notch radius, shape, depth etc., although analytical solution of every problem is almost impossible, due to complex boundary conditions and shapes.

iii) Numerical Methods

In recent years engineers have started using computer simulations based on finite elements analysis. The numerical methods have become the ultimate choice by the researchers in the last few decades, due to the galloping improvement of computing machines and programs and also due to the disadvantages of experimental and analytical methods that we referred previously.

We will examine analytical methods and FEM analysis, in more detail, in later chapters.

1.2. Shaft Materials

The selection of materials and the processes used in fabrication are integral parts of the design of any machine component. The materials used for manufacturing shafts vary, depending on their geometric characteristics and the loads they carry. In general, they must have the following properties:

1. High strength
2. Good machinability
3. Desired heat treatment properties
4. High wear resistance

Shafts are usually made of low carbon, cold drown or hot-rolled steel such as AISI 1020-1050 steels. Treatments like cold working and heat treatment are followed to give low carbon steels the necessary strength to resist loading stresses. The AISI 1020-1050 strength characteristics are given below in Table 1.

1	2	3	4	5
UNS No.	SAE and/or AISI No.	Process-ing	Tensile Strength, MPa (kpsi)	Yield Strength, MPa (kpsi)
G10200	1020	HR	380 (55)	210 (30)
		CD	470 (68)	390 (57)
G10300	1030	HR	470 (68)	260 (37.5)
		CD	520 (76)	440 (64)
G10350	1035	HR	500 (72)	270 (39.5)
		CD	550 (80)	460 (67)
G10400	1040	HR	520 (76)	290 (42)
		CD	590 (85)	490 (71)
G10450	1045	HR	570 (82)	310 (45)
		CD	630 (91)	530 (77)
G10500	1050	HR	620 (90)	340 (49.5)

Table 1 Tensile and yield strength for AISI 1020-1050 hot-rolled (HR) and cold-drawn (CD) low carbon steels. **[5]**

Although, heat treatment and high alloy content sometimes doesn't ensure significant strengthening. Fatigue failure is reduced moderately by increase in strength and only to a certain level, before adverse effects in endurance limit and notch sensitivity begin to counteract the benefits of higher strength. A good practice is a preliminary choice with inexpensive, low or medium carbon steel for the initial time through the design calculations. If strength considerations turn out to dominate over deflection, then a higher strength material should be tried. Nickel, nickel-chromium or chromium-vanadium alloys are often used for this purpose. This will allow the shaft sizes to be reduced until excess deflection becomes an issue. In this case, the cost of the material and its processing should be taken under consideration. When warranted, typical alloy steels for heat treatment include AISI 1340-50, 3140-50, 4140, 4340, 5140, and 8650. Shafts usually do not need to be surface hardened unless they serve as the actual journal of a bearing surface. Typical material choices for surface hardening include carburizing grades of AISI 1020, 4320, 4820, and 8620.

Cold drawn steel is usually used for diameters under about 3 inches. The nominal diameter of the bar can be left unmachined in areas that do not require fitting of components. Hot rolled steel should be machined all over. For large shafts requiring much material removal, the residual stresses may tend to cause warping. If concentricity is important, it may be necessary to rough machine, then heat treat to remove residual stresses and increase the strength, then finish machine to the final dimensions. In approaching material selection, the amount to be produced is a salient factor. For low production, turning is the usual primary shaping process. An economic viewpoint may require removing the least material. High production may permit a volume conservative shaping method (hot or cold forming, casting), and minimum material in

the shaft can become a design goal. Cast iron may be specified if the production quantity is high, and the gears are to be integrally cast with the shaft.

Properties of the shaft locally depend on its history-cold work, cold forming, rolling of fillet features, heat treatment, including quenching medium, agitation, and tempering regimen. Stainless steel may be appropriate for some environments [5].

1.3. Shaft Design for Stresses

Since shafting is so widely found in all types of machinery and mechanical equipment, its design may be the most frequently encountered task. In order to design a shaft, a mechanical engineer must take under consideration of the stress developing in shafts. There are always some locations in the shaft, which are prone to high stresses and therefore to failure (static or dynamic). Those usually appear on the outer surface at axial locations, where the bending moment is large and the torque is present and are called critical locations. The critical locations should be identified in order to avoid stress concentration factors. Therefore, the best way to identify the critical locations and design a shaft is to perform a stress analysis (by using one of the methods referred in the previous paragraph) and compare various points throughout the length of the shaft.

Most shafts transmit torque through a portion of their length. Typically, the torque comes into the shaft at one gear and leaves the shaft at another gear. A free body diagram of the shaft allows the torque at any section to be determined. The torque is often relatively constant at steady state operation, so that the shear stress due to the torsion takes its maximum values on outer surfaces.

The ‘‘equivalent’’ moments on a shaft can be determined by two-dimensional shear and bending moment diagrams [6], since most shaft problems incorporate gears or pulleys that introduce forces in two planes. Resultant moments are obtained by summing moments as vectors at points of interest along the shaft. The phase angle of the moments is not important since the shaft rotates, and this makes the problem a ‘‘fully-reversed’’ load case. This term means that a steady bending moment will produce a completely reversed moment on a rotating shaft, as a specific stress element will alternate from compression to tension in every revolution of the shaft. The normal stress due to bending moments will be greatest on the outer surfaces. In situations where a bearing is located at the end of the shaft, stresses near the bearing are often not critical since the bending moment is small.

Axial stresses on shafts due to the axial components transmitted through helical gears or tapered roller bearings will almost always be negligibly small compared to the bending moment stress. They are often also constant, so they contribute little to fatigue. Consequently, it is usually acceptable to neglect the axial stresses induced by the gears and bearings when

bending is present in a shaft. If an axial load is applied to the shaft in some other way, it is not safe to assume it is negligible without checking magnitudes. [5]

1.4. Shaft Stresses

Bending, torsion and axial stress may be present together in both midrange and alternating components. To calculate the stresses and perform a stress analysis, it is simply enough to combine the different types of stresses by Von Mises. Axial loads are usually very small at critical locations, because bending and torsion are dominate, so they are not taken into consideration. The stresses due to bending and torsion are given by the following equations:

$$\sigma_\alpha = K_f \frac{M_a c}{I} \qquad \text{Eq. 1} \qquad \sigma_m = K_f \frac{M_m c}{I} \qquad \text{Eq. 3}$$

$$\tau_\alpha = K_{fs} \frac{T_a r}{J} \qquad \text{Eq. 2} \qquad \tau_m = K_{fs} \frac{T_m r}{J} \qquad \text{Eq. 4}$$

Where M_m and M_a are the midrange and alternating bending moments, T_m and T_a are the midrange and alternating torques, and K_f and K_{fs} are the fatigue stress-concentration factors for bending and torsion, respectively.

Assuming for a solid shaft with round cross section, appropriate geometry terms can be introduced for c, I, r and J resulting in:

$$\sigma_\alpha = K_f \frac{32 M_\alpha}{\pi d^3} \qquad \text{Eq. 5} \qquad \sigma_m = K_f \frac{32 M_m}{\pi d^3} \qquad \text{Eq. 7}$$

$$\tau_\alpha = K_{fs} \frac{16 T_\alpha}{\pi d^3} \qquad \text{Eq. 6} \qquad \tau_m = K_{fs} \frac{16 T_m}{\pi d^3} \qquad \text{Eq. 8}$$

Note that for a rotating shaft with constant bending and torsion, the bending stress is completely reversed and the torsion is steady. So, the equations above can be simplified by setting M_m and T_a equal to 0, which simply drops out some of the terms. [5]

1.5. Stress raisers and relief grooves

Most service failures in shafts are attributable largely to some condition that causes stress intensification. An apparently insignificant imperfection such as a small surface irregularity may

severely reduce the strength of a shaft, if the stress level at the imperfection is high. The most vulnerable zone in torsional and bending fatigue is the shaft surface, an abrupt change of surface configuration may have a damaging effect, depending on the orientation of the discontinuity to the direction of stress.

Stress-raisers are sharp corners, grooves, notches, or acute changes of cross-section that cause stress concentrations under normal loadings. As general rule, stress should be transmitted among the element without breaking some critical values and as smoothly as possible. “Predicting” the stress flow in mechanical structures can help avoiding such fatal damages.

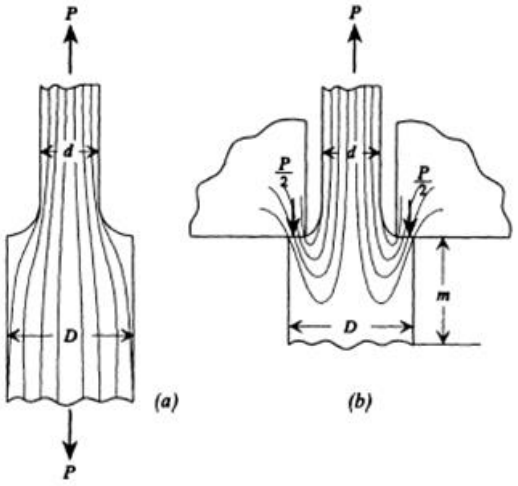

Figure 5 (a) A smooth stress flow (b) Sharp change in the stress flow that can cause higher stress allocation

In the circumstances where the stress raisers are necessitated by the functional requirements, the geometrical discontinuities should be placed in areas where the nominal stress load in the minimum. In Figure 5 (a) A smooth stress flow (b) Sharp change in the stress flow that can cause higher stress the stress flow is highly affected by the sharp changes of the geometry. Both parts have the same shape but totally different stress levels.

In cases where it is necessary, sharp transitions should be removed from the surface of the element in order to ensure a uniform stress flow. Stress concentrations at notches and grooves can be reduced by the "metal removal – stiffness reduction" technique utilizing any procedure which improves the stress flow, e.g. multiple notches of U grooves and selected hole drilling as shown in Figure 6Figure 6 Various procedures for the reduction of stress concentrations at notches or grooves , or shoulders, large radius undercuts and relief grooves as shown in Figure 7 Large radious undercuts, shoulders and notches used to achieve a smoother stress Figure 7. Therefore, reductions of the order of 30% can be obtained.

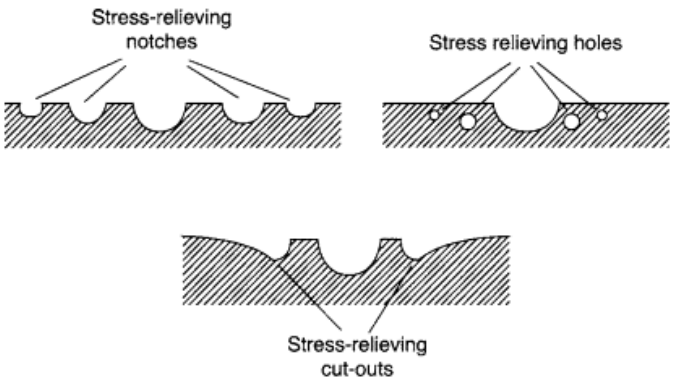

Figure 6 Various procedures for the reduction of stress concentrations at notches or grooves [7]

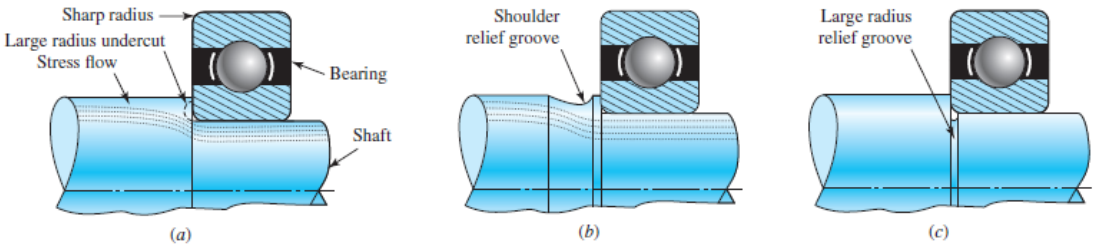

Figure 7 Large radious undercuts, shoulders and notches used to achieve a smoother stress [5]

Note that additional notches, like those shown in Figure 6, should be placed in series and not in parallel, otherwise the results in stress concentration may be the opposite of the expected.

Chapter 2

2.1 Stress Concentration Factor

Stresses at or near a discontinuity, such as a sharp groove on a shaft, a shoulder on a shaft or a hole in a bar (as shown in Figure 8), are higher than if the discontinuity does not exist. Any such discontinuity alters the stress distribution, so that the elementary stress equations no longer describe the stress in the part. Therefore, failure will first occur at the discontinuity, which we generally call a stress raiser, as it will be the first part of the structure where concentrated stresses can exceed the material's strength. It should be noted that the real fracture strength of a material is always lower than the theoretical value, because most structural components contain discontinuity in geometry or joints which induces the stress concentration.

Figure 8 Stress distribution in plate with a hole subjected to axial loading [8]

The stress concentration is the region on a part where stress raisers are present and can be measured by the Stress Concentration Factor (SCF). In more detail, the stress concentration factor, K_t, is the factor used to relate the actual maximum stress at the discontinuity to the average of the nominal stress. SCF characterizes as a function of; a geometry or shape of the part but not its size or material, type of loading applied to the part (axial, bending and torsional), specific geometric raiser on the part (fillet radius, notch or hole) and always defined with respect to a particular nominal stress and assumes a linear, elastic, homogenous, isotropic material. [5]

The SCF allows consideration of stress raisers without excessively complicating the mathematics. The value of K_t is usually determined by some experimental method, such as photoelastic analysis of the plastic model of a part, or by analytical or numerical simulation of the stress field, as we already have discussed in Chapter 1.

2.2 Selection of Nominal Stresses

As shown by the definition of K_t, SCF is dimensionless and it is defined as the ratio of the peak stress in the body to some other stress taken as a reference normal stress.

$$K_t = \frac{\sigma_{max}}{\sigma_{nominal}} \quad for\ normal\ stress\ (tension\ or\ bending)$$

Eq. 9

$$K_{ts} = \frac{\tau_{max}}{\tau_{nominal}} \quad for\ shear\ stress\ (torsion)$$

Eq. 10

In the cases of a bar with circular cross section with u-shaped groove subjected to tension, bending and torsion, like the cases shown in Figure 9 the nominal stresses are given by the following equations relatively:

$$\sigma_{nomt} = \frac{4 \times P}{\pi \times (D - 2h)^2} \quad for\ axial\ load$$

Eq. 11

$$\sigma_{nomb} = \frac{32 \times M}{\pi \times (D - 2h)^3} \quad for\ bending\ load$$

Eq. 12

$$\tau_{nom} = \frac{16 \times T}{\pi \times (D - 2h)^3} \quad for\ torsional\ load$$

Eq. 13

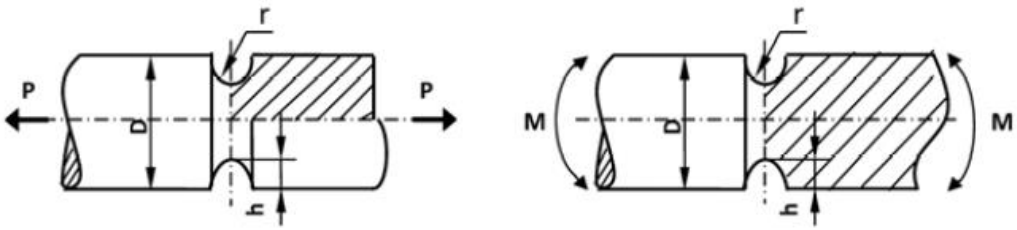

Figure 9 Bar of circular cross section with u-shaped groove subjected to tension and bending [9]

Therefore, it is well understood that the expression of the reference stresses σ_{nom} that is used depends on the respective problem and it is very important for the engineer to be able to properly identify the reference stress for the purpose of calculating the stress concentration factor. The example below should help to explain the selection of the nominal stress.

Example 1 Tension bar with a groove [4]

A bar of circular cross section, with a U-shaped circumferential groove, is subjected to an applied torque T. The diameter of the bar is D, the radius of the groove is r, and the depth of the groove is t. The stress distribution for the cross section at the groove is shown in Figure 10, with the maximum stress occurring at point A at the bottom of the groove. The reference stress could be defined in the following ways:

(1) Use the stress at the outer surface of the bar cross section B'-B', which is far from the groove, as the reference stress. According to basic strength of materials (Pilkey 2005), the shear stress is linearly distributed along the radial direction and

$$\tau_{B'} = \tau_D \frac{16T}{\pi D^3} = \tau_{nom}$$

Eq. 14

(2) Consider point A' in the cross section B'-B'. The distance of A' from the central axis is same as that of point A, that is, $d = D - 2t$. If the stress at A' is taken as the reference stress, then

$$\tau_{A'} = \frac{16Td}{\pi D^4} = \tau_{nom}$$

Eq. 15

(3) Use the surface stress of a grooveless bar of diameter $d = D - 2t$ as the reference stress. This corresponds to a bar of cross section measured at A-A of Figure 10. For this area πd2/4, the maximum torsional stress taken as a reference stress would be

$$\tau_A = \frac{16T}{\pi D^3} = \tau_{nom}$$

Eq. 16

In fact this stress based on the net area is an assumed value and never occurs at any point of interest in the bar with a U-shaped circumferential groove. However, since it is intuitively appealing and easy to calculate, it is used more often than the other two reference stresses.

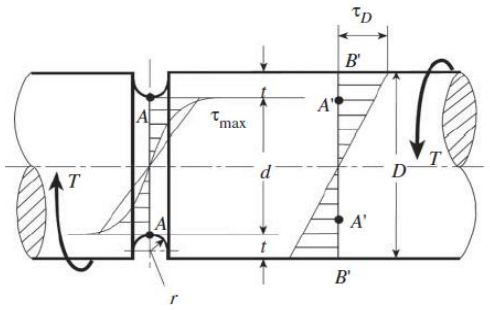

Figure 10 Example of determining nominal stress (bar with u-shaped groove subjected to torsion)

2.3 Theoretical Stress Concentration Factor

The first mathematical treatments of stress concentration were published shortly after 1900. Experimental methods for measuring high localized stresses were developed and used, in order to handle other than very simple cases. Nowadays, finite element studies with the help of modern computing machines have also been employed. The results of many of these previous studies are available thanks to R.E. Peterson who compiled them in form of tables and published graphs, such as the following Figure 11. Peterson also developed the style of presentation in which the stress concentration factor K_t is multiplied by the nominal stress σ_{nom}, in order to estimate the magnitude of the maximum stresses in the specimen.

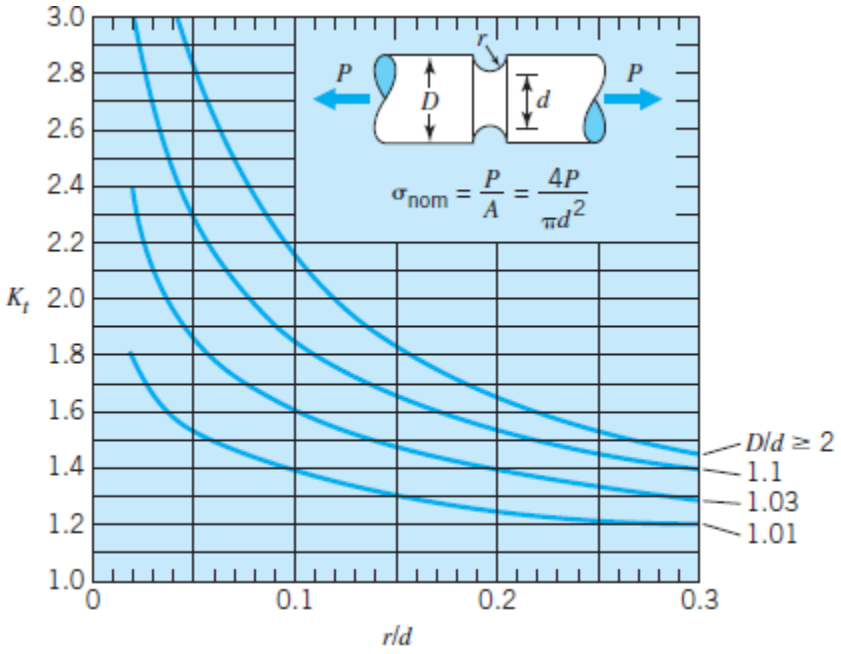

Figure 11 Typical graph for a shaft with u-shaped groove under axial loading [10]

At this point, it should be emphasized that the stress concentration factors given in graphs are theoretical or, even better, geometric factors based on a theoretical homogeneous, isotropic and elastic material. Real materials and real mechanical parts have microscopic irregularities (from processing and use) that can be considered as extremely small notches and causing a certain nonuniformity of microscopic stress distribution.

More present mathematical models can also give a good approximation of the theoretical stress concentration factor, like the expression below:

$$K_t = C_1 + C_2 \left(\frac{2t}{D}\right) + C_3 \left(\frac{2t}{D}\right)^2 + C_4 \left(\frac{2t}{D}\right)^3 \quad [9] \qquad \text{Eq. 17}$$

where, for tension,

$$C_1 = 0.89 + 2.208\sqrt{t/r} - 0.094\, t/r \qquad \text{Eq. 18}$$

$$C_2 = -0.923 - 6.678\sqrt{t/r} + 1.638\, t/r \qquad \text{Eq. 19}$$

$$C_3 = 2.893 + 6.448\sqrt{t/r} - 2.516\, t/r \qquad \text{Eq. 20}$$

$$C_4 = -1.912 - 1.944\sqrt{t/r} + 0.963\, t/r \qquad \text{Eq. 21}$$

Considering the geometry of the problem, it appears that $r = \frac{D-d}{2}$ and this leads to t/r=1. Therefore the values of C_1, C_2, C_3 and C_4 are:

C_1= 3.004, C_2= 7.393, C_3= -6.071, C_4= -2.893

2.4 Notch Sensitivity

As already referred, the theoretical stress concentration factors apply mainly to ideal elastic materials and depend on the geometry of the body and the loading, yet there are cases where a more realistic model is needed. When the applied loads reach a certain level, plastic deformations may be involved and the actual strength of structural members may be quite different from that derived using theoretical stress concentration factors, especially for the cases of impact and alternating loads. Therefore, it is reasonable to introduce the concept of the *effective stress concentration factor* K_e, also referred as the notch rupture strength ratio. The magnitude of K_e is obtained experimentally. For instance, K_e for a round bar with a circumferential groove subjected to a tensile load P' (Figure 12) is obtained as follows:

1. Two sets of specimens of the actual material, the round bars of the first set having circumferential grooves, with d as the diameter at the root of the groove (Figure 12a). The round bars of the second set are of diameter d without grooves (Figure 12b).

2. In a tensile test for the two sets of specimens, the rupture load for the first set is P', while the rupture load for second set is P.

3. The effective stress concentration factor is defined as:

$$K_e = \frac{P}{P'} \qquad \text{Eq. 22}$$

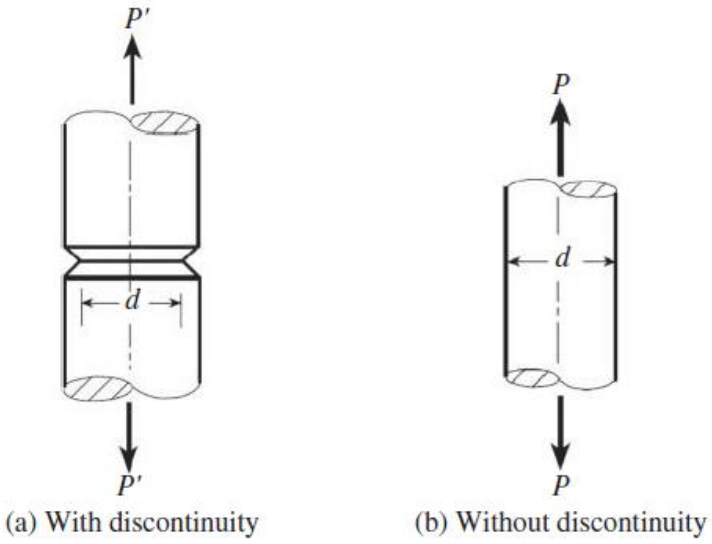

Figure 12 Specimens for obtaining K*e*

In general, $P^{'} > P$ so that $K_e > 1$. The effective stress concentration factor is a function not only of geometry but also of material properties. Some characteristics of K_e for static loading of different materials are discussed briefly below.

1. Ductile material. A tensile loaded plane element with a V-shaped notch. The material law for the material is sketched in Figure 13. If the maximum stress at the root of the notch is less than the yield strength $\sigma_{\max} < \sigma_y$ the stress distributions near the notch would appear as in curves 1 and 2 in Figure 13. The maximum stress value is:

$$\sigma_{\max} = K_t \sigma_{nom}$$

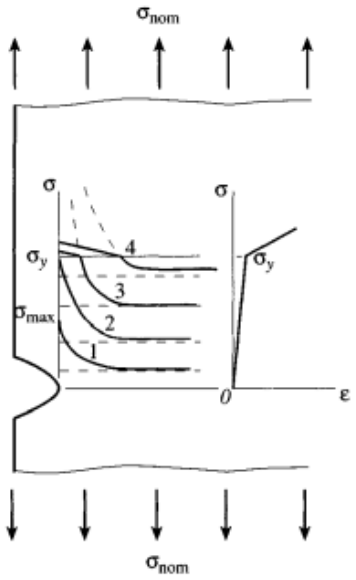

Figure 13 Stress distribution near a notch for a ductile material. [4]

As the $\sigma_{\max}$ exceeds σ_y, the strain at the root of the notch continues to increase but the maximum stress increases only slightly. The stress distributions on the cross section will be of the form of curves 3 and 4 in Figure 13, so the equation above no longer applies to this case. As σ_{nom} continues to increase, the stress distribution at the notch becomes more uniform and the effective stress concentration factor K_e is close to unity.

2. Brittle material. Most brittle materials can be treated as elastic bodies. When the applied load increases, the stress and strain retain their linear relationship until damage occurs. The effective stress concentration factor K_e is the same as K_t .

3. Gray cast iron. Although gray cast irons belong to brittle materials, they contain flake graphite dispersed in the steel matrix and a number of small cavities, which produce much higher stress concentrations than would be expected from the geometry of the discontinuity. In such a case the use of the stress concentration factor K_t may result in significant error and K_e can be expected to approach unity, since the stress raiser has a smaller influence on the strength of the member than that of the small cavities and flake graphite.

It can be reasoned from these three cases that the effective stress concentration factor depends on the characteristics of the material and the nature of the load, as well as the geometry of the stress raiser. Also $1 \le K_e \le K_t$. The maximum stresses at rupture can be defined to be:

$$\sigma_{\max} = K_e \sigma_{nom} \qquad \text{Eq. 23}$$

To express the relationship between K_f and K_t , introduce the concept of notch sensitivity (Boresi 1993):

$$q = \frac{K_e - 1}{K_t - 1} \qquad \text{Eq. 24}$$

Or

$$K_e = q(K_t - 1) + 1 \qquad \text{Eq. 25}$$

And the can be defined as:

$$\sigma_{\max} = \left[q(K_t - 1) + 1\right]\sigma_{nom} \qquad \text{Eq. 26}$$

If $q = 0$, then, $K_e = 1$ meaning that the stress concentration does not influence the strength of the structural member. If $q = 1$, then $K_e = K_t$ implying that the theoretical stress concentration factor should be fully invoked. The notch sensitivity is a measure of the agreement between K_e and K_t . The concepts of the effective stress concentration factor and notch sensitivity are used primarily for fatigue strength design. For fatigue loading:

$$K_f = \frac{\textit{Fatigue}\ \text{limit of unnotched specimen(axial or bending)}}{\textit{Fatigue}\ \text{limit}\ \textit{of}\ \text{notched specimen(axial or bending)}} = \frac{\sigma_f}{\sigma_{nf}} \qquad \text{Eq. 27}$$

$$K_{fs} = \frac{\textit{Fatigue}\ \text{limit of unnotched specimen(shear stress)}}{\textit{Fatigue}\ \text{limit}\ \textit{of}\ \text{notched specimen(shear stress)}} = \frac{\tau_f}{\tau_{nf}} \qquad \text{Eq. 28}$$

Where K_f is the fatigue notch factor for normal stress and K_{fs} is the fatigue notch factor for shear stress, such as torsion. The notch sensitivities for fatigue become:

$$q = \frac{K_f - 1}{K_t - 1} \qquad \text{Eq. 29}$$

or

$$q = \frac{K_{fs} - 1}{K_{ts} - 1} \qquad \text{Eq. 30}$$

The values of q vary from $q = 0$ for no notch effect ($K_f = 1$) to $q = 1$ for the full theoretical effect ($K_f = K_t$).

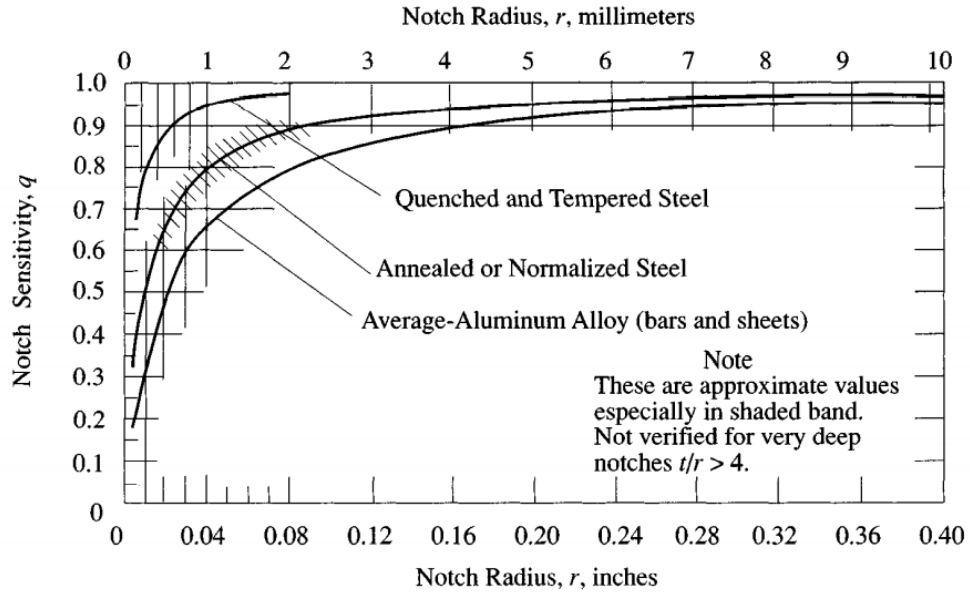

Figure 14 Average fatigue notch sensitivity [10].

Where K_{tf} is the estimated fatigue notch factor for normal stress, a calculated factor using an average q value obtained from Figure 14 or a similar curve, and K_{tsf} is the estimated fatigue notch factor for shear stress.

2.5 Influence of Poisson's Ratio on K_t

In general stress concentration factors will change with different materials. Poisson's ratio *v* is often involved in a three-dimensional stress concentration analysis and modern charts for three dimensional stress concentration problems not only list the body shape and load, but also specify the Poisson's ratio v for the case. Althought, many original charts made from photoelastic expirements do not include the value of v.

The influence of Poisson's ratio on the SCF varies with the configuration. For example, in the case of a circumferential groove in a round bar under torsional load the stress distribution and concentration factor do not depend on v. This is because the shear deformation due to torsion does not change the volume of the element, namely the cross-sectional areas remain unchanged.

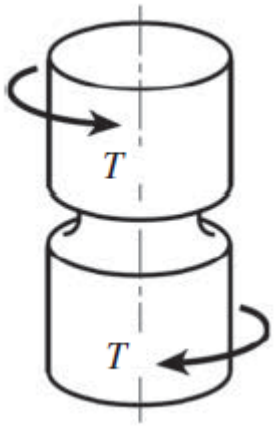

Figure 15 Round bar with a circumferential groove under torsion

In Dally & Riley (1991) it is stated that the influence from Poisson ratio on the result is usually small, meaning less than 7%. There isn't much information found in literature for the influence of Poisson's ratio on Kt for a shaft with a U-shaped circumferential groove under tension, but in general the influence of v increases for the low values of r/d and is smaller as the r/d ratio decreases.

In the previous part of the paper when not specified and in the remaining part of the paper we will assume that $v = 0,3$ corresponding to the normal value for a steel shaft.

Chapter 3

3.1 Finite Elements Method

Finite Elements Method (FEM) is the fastest and most effective method that engineers use nowadays in order to analyze and solve a wide range of problems, both linear and non-linear problems (strain-displacement) of continuous parts. While it is difficult to quote a date of the invention of the finite element method, the method originated from the need to solve complex elasticity and structural analysis problems in civil and aeronautical engineering. Engineering structures that have complex geometry and loads, are either very difficult to analyze or have no theoretical solution. However, in FEA, a structure of this type can be easily analyzed and the user can solve a complex engineering problem without knowing the governing equations or the mathematics; the user is required only to know the geometry of the structure and its boundary conditions.

Finite element analysis (FEA) involves solution of general field engineering problems, like elasticity, fluid flow, heat transfer problems, etc. using various professional programs, such as Abaqus, ANSYS, ALGOR and NASTRAN. In this technique the structure is divided into very small but finite size elements (hence the name finite element analysis). Individual behavior of these elements is known and, based on this knowledge the behavior of the entire structure can be determined (Figure 16). The relationships that are used and the properties of the materials are considered on these elements and are expressed in terms of uknown values in their angles which respond in relation to the finite element and are colled its nodes.

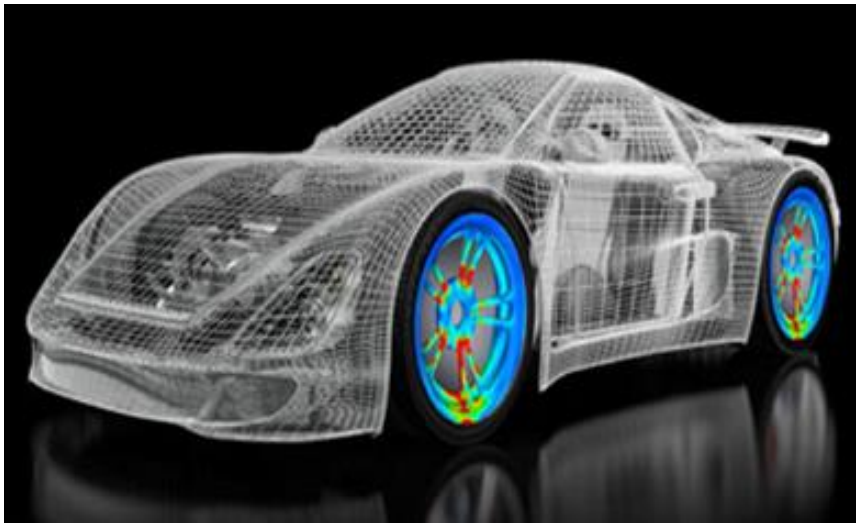

Figure 16 The frame of a car divided into finite elements [11]

Numerical stress analysis with the Finite Elements Method can give accurate results of stresses developing in discontinuity and as a result, the use of SCF is nowadays unnecessary. Although, we can first calculate the SCF with the help of the numerical study and use it later for the design of mechanical structures with more classical methods.

3.2 FEM Modeling Shafts

Static strength evaluation of components and machine elements (such as shafts) makes the modelling and estimation of stress concentrations very important. This evaluation demands a high number of FEM meshing nodes on the boundary shape where the stress concentration is present. For a given design, the position of high stress can be found and the element refinement can be done locally at this specific position, reducing the need for overall mesh refinement considerably. In optimization, where the reduction of maximum strenght is the purpose, the point of maximum stress is not known but is a function of the design. In fact, the optimality criterion for minimum stress on the surface is that the stress is constant on the surface, which will increase the number of nodes on the boundary since we need to evaluate the stress over a larger area.

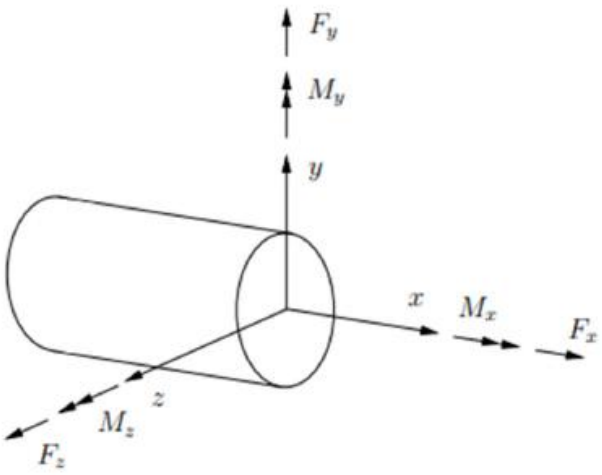

Figure 17 Definitions of forces and moments on a beam cross section

In Figure 17 the possible forces and moments on a shaft are shown, axial load F_x , torsional load M_x. The bending moment is $Mb = \sqrt{My^2 + Mz^2}$. The total shear force $Fs = \sqrt{Fz^2 + Fy^2}$ is normally not accounted for because the shear stress associated with this force is zero at the point of maximum normal stress due to the bending moment. The shaft geometry is axisymmetric and only the axial load is also axisymmetric. FEM modeling of the shaft can be done in many ways. For the axial load the simplest modeling is to use a standard axisymmetric model. For torsional load, the loading is out-of-plane relative to the plane of a 2D axisymmetric model, and this cannot be done with standard axisymmetric modeling. A full 3D shaft modeling can of course be used but due to the symmetry we can reduce the 3D model to a sector of a circle where the central angle in principle can go to zero, but this will be limited by the resulting FEM mesh quality. [12]

3.3 Diploma Thesis

A common problem in any mechanical construction is the determination of the stress load that develops, as well as the definition of the critical values that can cause a possible failure. Almost every mechanical structure consists of shafts which are designed with geometrical discontinuities that receive the highest values of stresses. A common type of discontinuity is the circumferential grooves or notches, particularly U-shaped notches, that occur frequently in engineering design in such applications as C-ring retainer grooves, oil grooves, shoulder or grinding relief grooves, seal retainers, etc. [7]. We consider a shaft that the initial diameter D decreases to a smaller diameter d due to a U-shaped circumferential groove with radius r.

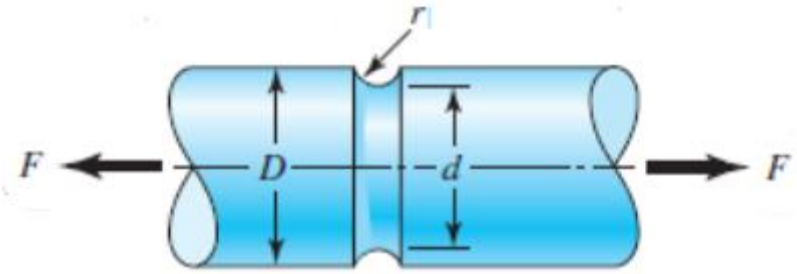

Figure 18 Diploma thesis shaft

These geometrical discontinuity causes stress concentration in discontinuous regions. The stress concentration factor K_t, as discussed in the previous chapter, is the only parameter can be used in order to determine the stress load. The stress concentration factor is affected by a unique parameter and that is the geometry of the specimen. To be more specific, K_t is affected by the fraction of the groove radius to the inner diameter d *(r/d).* The calculation of the stress concentration factor with the Finite Elements Method and the comparison with the theoretical results found in literature is the main purpose of this project. For this experiment, it is assumed that the specimens are under tensile loads and the same procedure will be applied to four different geometries with the same length of *180 mm* shown in the table below (Table 2). This will also prove the dependence of the stress concentration factor to the fraction of r/d.

Specimen	D (mm)	d (mm)	r (mm)	D/d	r/d
3005	40	36.4	1.8	1.1	0.05
3075	40	34.7826	2.6087	1.15	0.075
3015	40	30.7692	4.6154	1.3	0.15
3025	40	26.6666	6.6667	1.5	0.25

Table 2 Geometrical features of the examined specimens

3.4 Defining the Two-Dimensional Axisymmetric Problem in Abaqus

This project is analyzed in the Abaqus environment. As the specimen has a cylindrical body, then cylindrical coordinates can be used (Figure 19). The body of the specimen possesses two axis of symmetry and the problem solution is independent of angle θ. Therefore the problem can be defined as axisymmetric and besides it is a three-dimensional problem, it can be "converted" to a two-dimensional one.

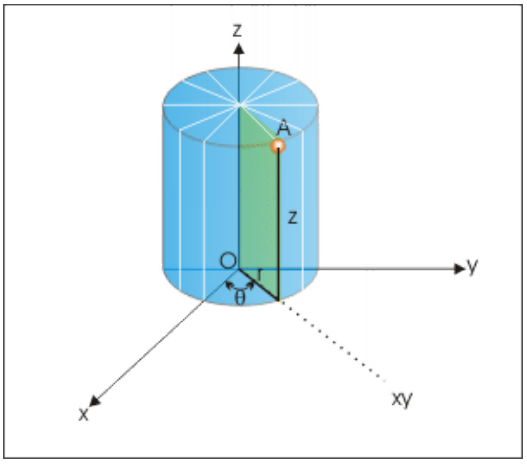

Figure 19 Cylindrical coordinates on a cylindrical body

The first step in order to design the specimens in Abaqus is to design the 2D problem by exploiting the double symmetry of the specimen and designing the ¼ of the specimen. Because both the geometry and loads are symmetric, the numerical simulation can be performed on only a portion of the whole model to reduce computation. Then, the border conditions and the loads will be applied. To be more specific, a tensile load will be applied to one end, while the other one will be anchored. In the last step the 3D domain will be designed by revolving the two-dimensional sketch around the axis of symmetry by 360 degrees.

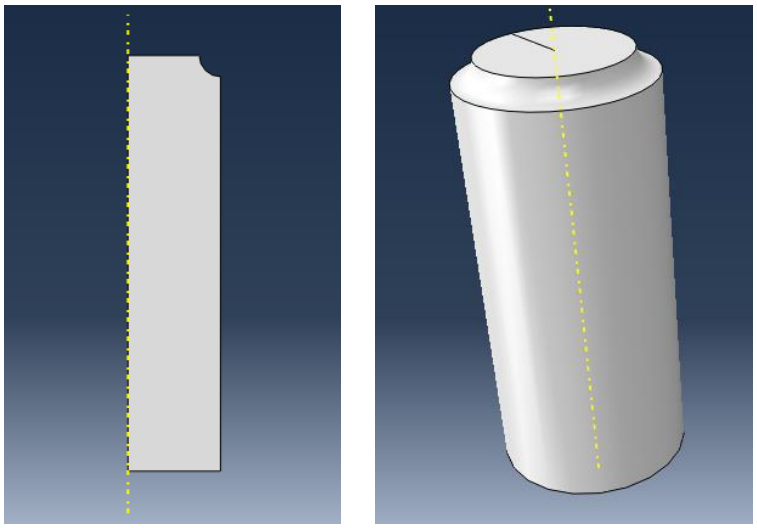

Figure 20 Axisymmetric part and 3D part of specimen 3015

3.5 Modeling the Axisymmetric Problem in Abaqus

3.5.1 Border Conditions

The simulation of border (or boundary) conditions and other forms of constraint is probably the single most difficult part of the accurate modelling of a structure for the Finite Element Analysis. Border conditions can be used to specify the values of all basic solution variables (displacements, rotations, warping amplitude, fluid pressures, pore pressures, temperatures, electrical potentials, normalized concentrations, acoustic pressures, or connector material flow) at nodes. In specifying constraints, it is relatively easy to make mistakes of omission or misrepresentation. It may be necessary for the analyst to test different approaches to model esoteric constraints such as bolted joints, welds, which are not as simple as the idealized pinned or fixed joints. Testing should be confined to simple problems and not to a large, complex structure. Sometimes, when the exact nature of a boundary condition is uncertain, only limits of behavior may be possible. For example, shafts with bearings have been modeled as being simply supported. It is more likely that the support is something between simply supported and fixed, and we could analyze both constraints to establish the limits. However, by assuming simply supported, the results of the solution are conservative for stress and deflections. That is, the solution would predict stresses and deflections larger than the actual.

Multipoint constraint equations are quite often used to model boundary conditions or rigid connections between elastic members. When used in the latter form, the equations are acting as elements and are thus referred to as rigid elements. Rigid elements can rotate or translate only rigidly, while boundary elements are used to force specific nonzero displacements on a structure. [5]

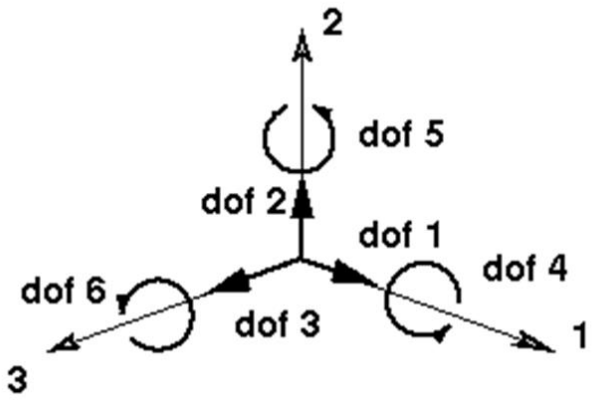

Figure 21 Displacements on all three direcrions

In Abaqus, boundary conditions correspond to specific degrees of freedom that are restrained. Except for axisymmetric elements, the degrees of freedom that are related to displacement and rotation in Abaqus, are referred to as follows :

1. Displacement in the 1 - axis (U1)
2. Displacement in the 2 - axis (U2)
3. Displacement in the 3 - axis (U3)
4. Rotation about the 1 - axis (UR1)
5. Rotation about the 2 - axis (UR2)
6. Rotation about the 3 - axis (UR3)

Axisymmetric elements use only four of the degrees of freedom above (U1, U2, UR2 and UR3).

Therefore, for this project specifically, the boundary conditions can be shown in Figure 22 in the next paragraph and are the following:

- The first border condition is applied at the axis of symmetry in the 1-direction.

$$U_1 = 0 \qquad \text{Eq. 31}$$

- The second border condition is applied on the “top” of the specimen.

$$U_2 = 0 \qquad \text{Eq. 32}$$

$$UR_3 = 0 \qquad \text{Eq. 33}$$

3.5.2 Tensile Load

One aspect that needs to be taken under consideration for applying loads is related to Saint-Venant’s principle. This means that the method in which the load is applied does not affect the stresses at a sufficient distance away from the load application location. So, if one is not concerned about the stresses near points of load application, there is no need to attempt to distribute the load very precisely. On the opposite, the analyst should not be impressed or concerned, when reviewing the results and the values of the stresses in the vicinity of the load application are found to be very large.

According to what is described above and for the geometry of the specimens examined in this project, if the load is applied at the top of the specimen which is very close to the region of interest (groove), then the calculations of the stress distribution turn out to be wrong. This can be fixed easily by applying the tensile load at the bottom of the specimen and border conditions at the top.

The value of the distributed tensile load is *100 MPa*. The first reason for that is that the calculations of K_t are easier, but the main reason should be considered to be for purposes of not reaching the critical value of the material.

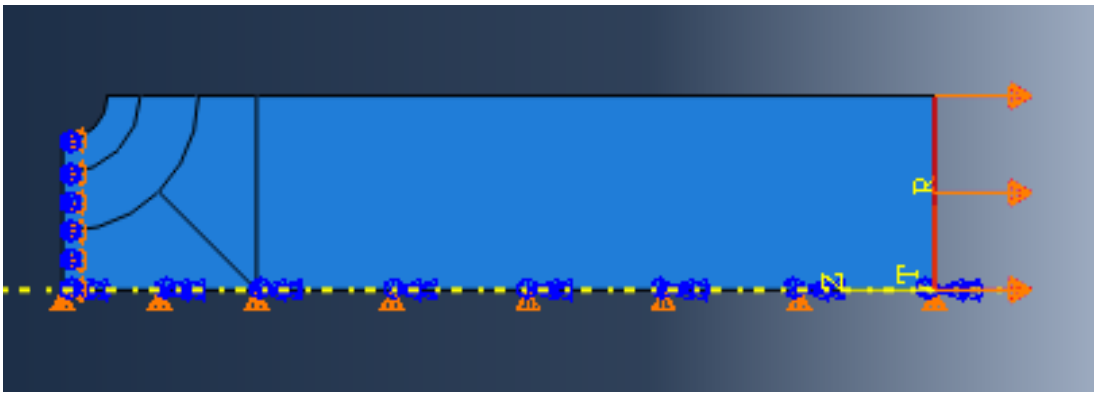

Figure 22 Border conditions and tensile load

3.5.3 Partitions and Meshing

The Finite element model in Abaqus is based both on nodes and elements that form a grid. That grid, or in other words, the network of nodes and elements that discretize a region of the model, is usually referred to as a mesh and all the users of programs like Abaqus must have a good knowledge and understanding about the mesh module's tools and settings in order to perform a stress analysis. There are three basic ways to generate an element mesh; manually, semi manually and automatically. For the specimens of this project the mesh construction became a semi-manually procedure, after many attempts.

Before meshing a part, it must be partitioned if needed. In the mesh module of Abaqus there are several kinds of tools for partitioning 2D and 3D parts. Note that meshing 3D parts is much more complex than partitioning 3D parts and needs more experience and that is the main reason of analysing the two dimensional model and then revolving it, as it was refered in the previous paragraph. The main reason for which the analyst creates partitions, is in order to have better control on the mesh pattern and the size of elements. This means that it is necessary for the mesh to be finer in the important regions (stress raisers including grooves, holes, cracks, fillets etc.), while there is no need for small elements in regions far from the stress raisers in order to get more accurate results, as seen in Figure 23 below. The partitions of the specimen are shown also shown in the same Figure 23.

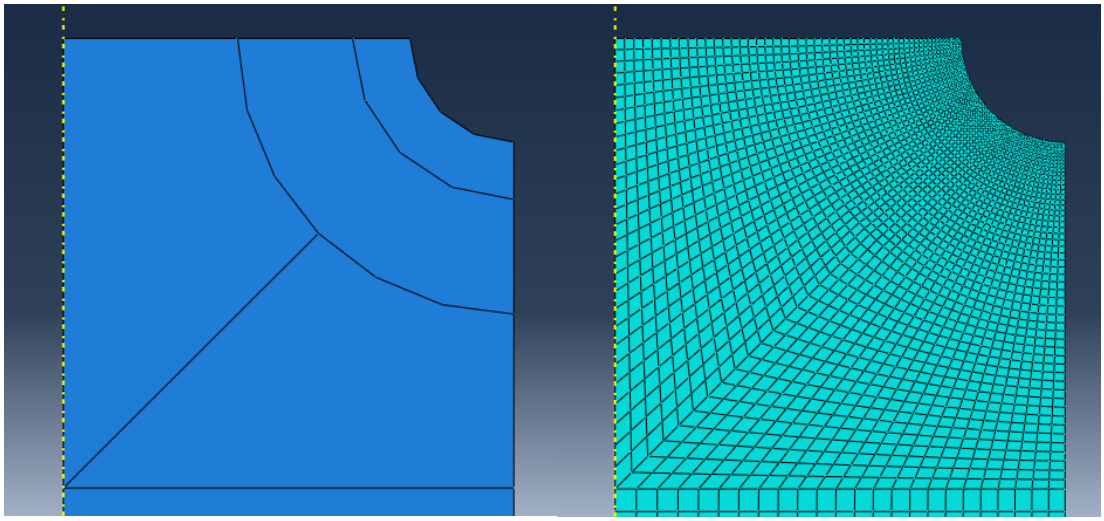

Figure 23 Partitions and meshing of specimen 3015

Also, the number of elements has an important effect on the simulation. Increasing the number of elements leads also to the increase of the simulation time and many times without any different result. Therefore, there is a great need for optimization of the mesh, meaning that the density of the mesh must be such that it is possible to approach accurate results with the least possible elements. This has a large effect on the simulation time. For example by optimizing the number of elements in large complicated models, the simulation time can be decreased from one day to several hours.

From the tests performed until the correct grid was achieved for the specimens of this project, it was observed that with the increase of the elements in the *r* direction we have a faster convergence towards the exact solution than if the elements in the θ direction increase (see Figure 24). In addition, the right size of the elements in the notch should be about one twentieth of the radius (r) of the curvature.

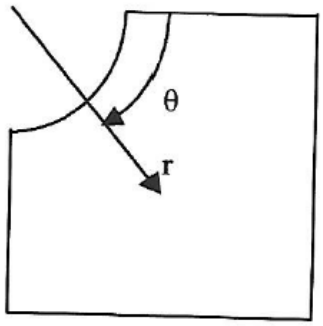

Figure 24 Possible directions of increasing the mesh density

It should also be mentioned that there was a need of designing a different grid for each specimen (therefore the whole procedure of meshing occurred semi-manually) and it was not

possible to use the same grid for all specimens. This is due to the fact that each specimen has a different radius of curvature resulting in an increase or decrease in the density of the grid in that area, giving wrong results and bad approximations of K_t. There was also no need of using the same number of elements for all the specimens, as this results to only a slightly different amount of time for each simulation.

3.6 Finite Elements in Abaqus – CAX4 Elements

Many geometric shapes of elements are used in Finite Analysis for specific applications. Abaqus utilizes an extensive element library to provide a powerful set of tools suitable for solving many different problems. Each element type has it's own advantages and limitations and selecting the appropriate element type is vitally important for obtaining accurate results.

In general, there are five aspects of an element that characterize its behavior in Abaqus and that one should consider when determining the optimal Abaqus element formulation for a given analysis:

- Family
- Degrees of freedom
- Number of nodes
- Formulation
- Integration

The *Element Family*, several of which are shown below (Figure 25), is used to describe the type of element and hint at applications for which it may be suitable. The major distinction between element families is the geometry type that each family assumes.

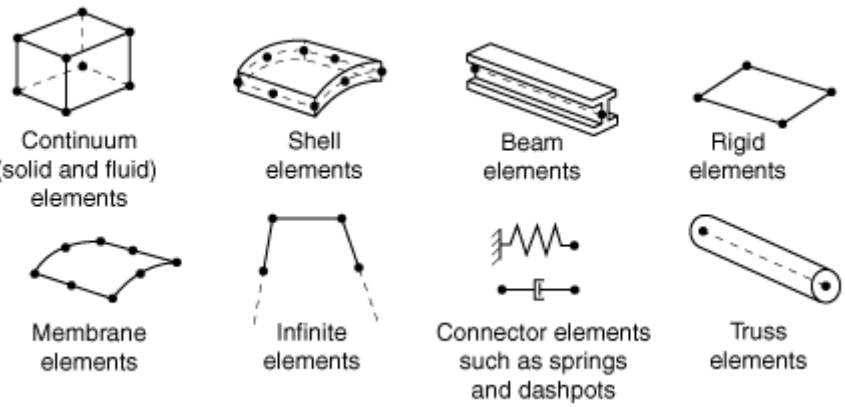

Figure 25 Commonly used element families

In addition, the *Number of nodes* that an element contains directly impacts the total *Degrees of freedom* and therefore has a significant impact on the element's ability to deform. Perhaps more importantly, the number of nodes an element has, dictates the strategy that will be used to interpolate the degrees of freedom calculated at the nodes to the rest of the element.

Within Abaqus, there are two available orders of interpolation: linear (elements that have nodes only at their corners) and quadratic (elements that have corner nodes and mid-side nodes).

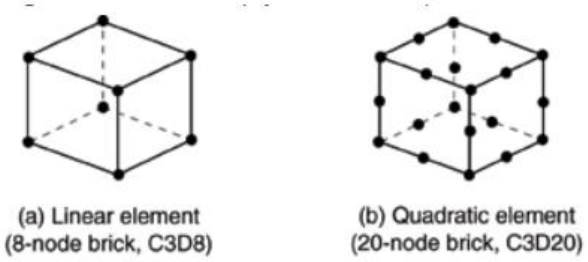

Figure 26 Linear and Quadratic elements

The *Formulation* of an element dictates the underlying mathematical algorithms governing element behavior. Fundamentally, there are two distinct types of elemental behavior: Lagrangian and Eulerian. The Langrangian model describes elements which deform with the material (appropriate for stress/displacement analyses), whereas Eulerian elements are fixed in space and allow material to flow through them (more suitable for representing fluid mechanics).

Last but no least, Abaqus uses *Integration* to determine various quantities throughout the volume of an element. The material response is evaluated at each of the integration points. Because each integration point requires mathematical resolution, it logically follows that elements with more integration points are computationally more expensive than those with fewer. To that end, several Abaqus element families provide a "Reduced Integration" option which uses fewer integration points than the standard element formulation. When used appropriately, reduced integration elements can substantially improve model efficiency and solver runtime. However, it must be noted that reduced integration elements have limitations which can lead to inaccurate results if used incorrectly.

According to the above and as found in Abaqus manual [13], the CAX4 Elements are the most suitable elements for modelling axisymmetric problems like the one in the present project. CAX4 is a 4-node bilinear, axisymmetric and solid (continuum) element, suitable for stress analysis as seen in Figure 27. The (r) and (θ) directions coinside with the global X and Y axis respectively. The structure is symmetric about the (z) axis. The concentrated loads are defined as the total loads integrated around the circumference, while the distributed loads should be provided as loads per unit of surface area. CAX4R (Reduced Integration) elements could be also suitable for this project but better approximations of K_t were achieved with the use of CAX4 elements.

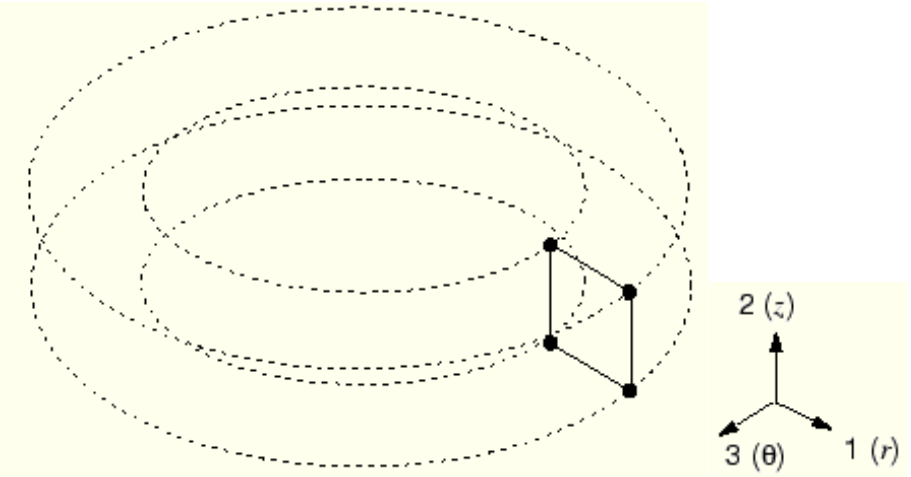

Figure 27 Axisymmetric element CAX4

3.7 Final Mesh and Stress Distribution

After the finite element analysis is completed with the help of Abaqus software, we can obtain a clear picture of the stress distribution on each one of the specimens. As we can observe from the following Figure 28 (28-31) of the 2D specimens, the location of the maximum stresses appears at the bottom of the u-shaped groove.

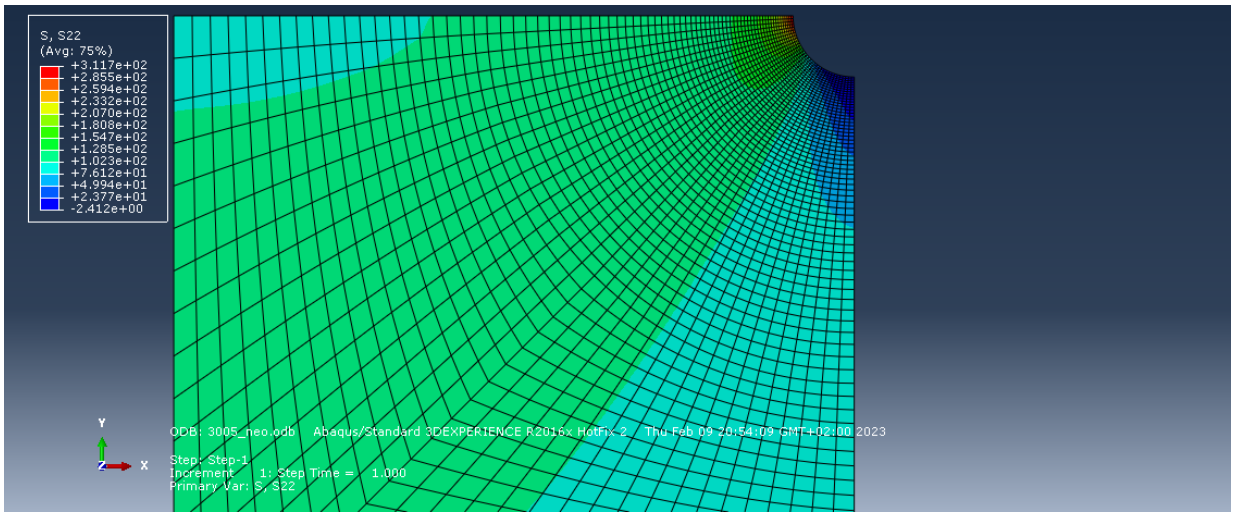

Figure 28 Stress distribution across the 3005 element in Abaqus CAE

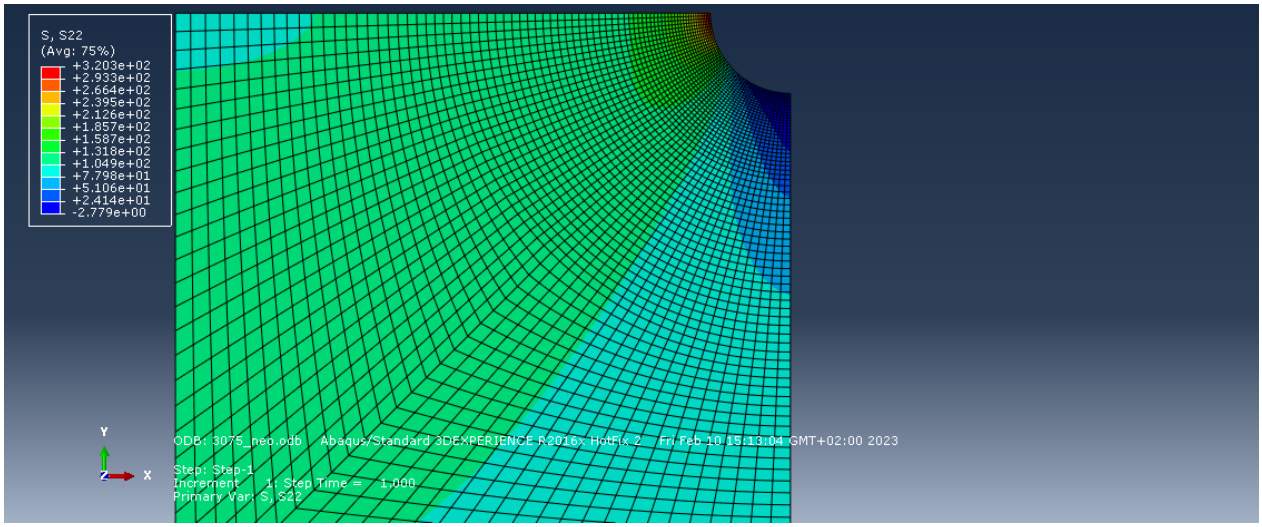

Figure 29 Stress distribution across the 3075 element in Abaqus CAE

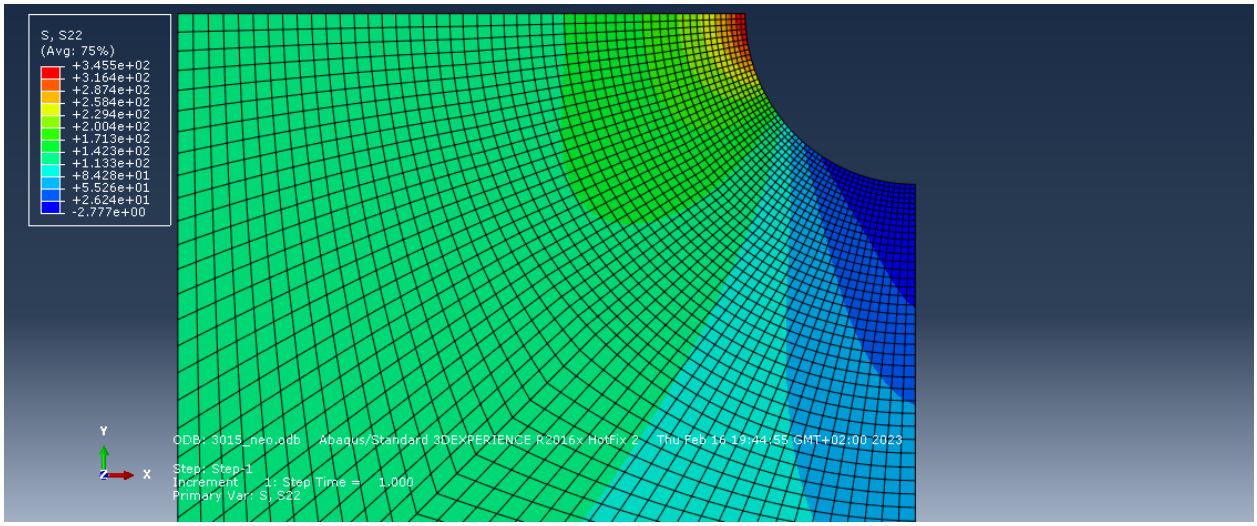

Figure 30 Stress distribution across the 3015 element in Abaqus CAE

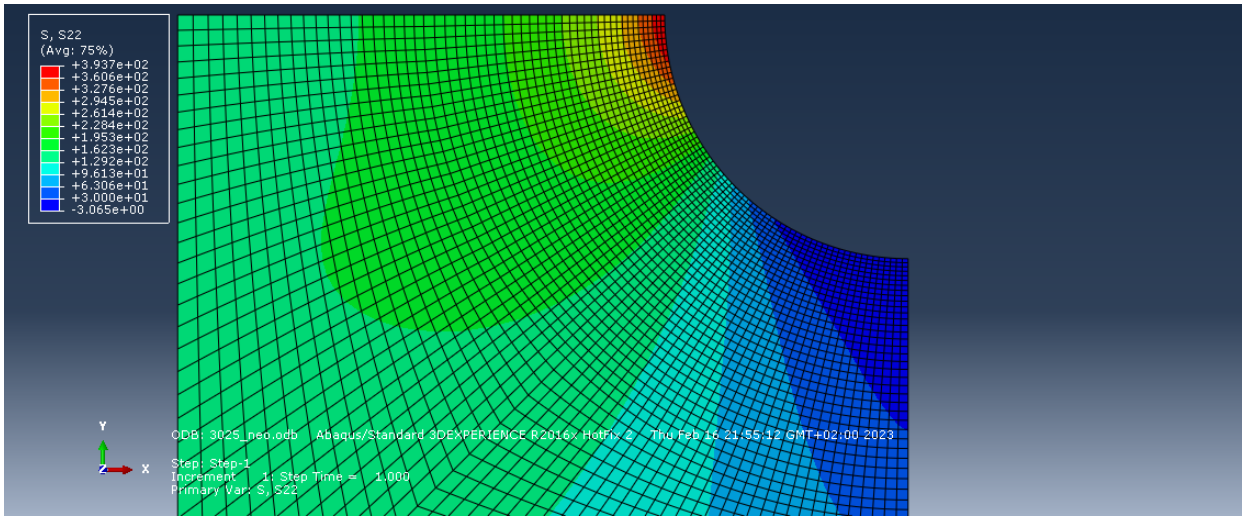

Figure 31 Stress distribution across the 3025 element in Abaqus CAE

By rotating the 2-D specimen by 360 degrees, we can obtain a 3-D view of the entire specimen. The results of the 3-D analysis are the same, meaning that the peak stresses appear at the bottom of the groove, as we can see in the following Figure 32.

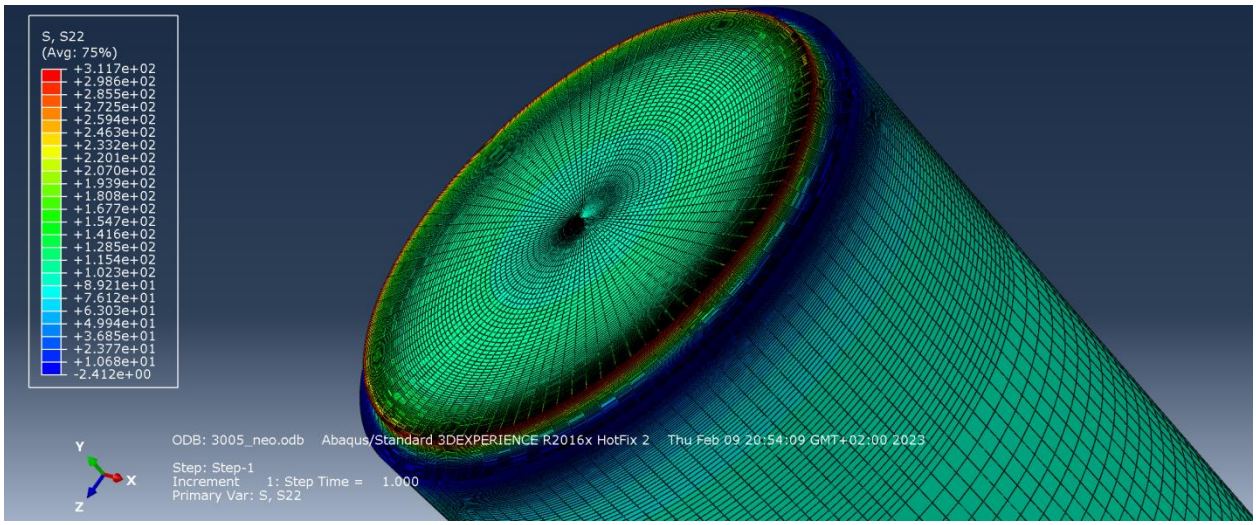

Figure 32 Stress distribution across the 3-D model of specimen 3005 in Abaqus environment

Chapter 4

4.1 FEM Analysis Results

As presented in the previous paragraph, after finishing the FEM analysis via Abaqus, the program gives the user the magnitudes of stresses across the whole model. The maximum value obtained can be used in order to calculate the stress concentration factor K_t from the following expression,

$$K_t = \frac{\sigma_{max}}{\sigma_{nominal}}$$

Eq. 34

Note that, as the same tensile load *σ=100MPa* is applied at the end of each specimen, then $\sigma_{nominal}$ at the inner diameter (d) of each specimen and in the center of the notch can be calculated as

$$\sigma_{nominal} = \sigma \times \frac{D^2}{d^2}$$

Eq. 35

The results for the four specimens, taken from the procedure described previously, are given accurately in the table below (Table 3) and their values can be compared with the values of K_t, as they are given by Peterson's diagrams.

Specimen	$\sigma_{nominal}$ (MPa)	$\sigma_{22,max}$ (MPa)	K_t Peterson	K_t FEM	Error %
3005	120.7584	311.7	2.6	2.581188	0.7236
3075	132.2501	320.3	2.47	2.421927	1.9463
3015	169.0003	345.5	2.08	2.044375	1.7128
3025	225.0011	393.7	1.78	1.749769	1.6984

Table 3 Abaqus results and stress comparison for specimens under examination

Note that there is an inverse relationship between the stress concentration factor K_t and the *r/d* ratio's value, while the relationship between K_t and the values of *D/d* ratios is positive.

The following Figure 33 shows the stress distribution (σ_{22}) for the specimen 3025 at the intersection made between the two antidiametric points located at the bottom of the notch. The red curve shows the stress distribution when the specimen of circular cross section has a constant diameter D=26,666 mm (without any groove) and the blue one shows the stress distribution for a shaft of round cross-section with outer diameter D=40 mm and a u-shaped

notch groove that reduces the diameter to its minimum value, which is d=26,666 mm. The horizontal axis shows the distance from the center of the intersection.

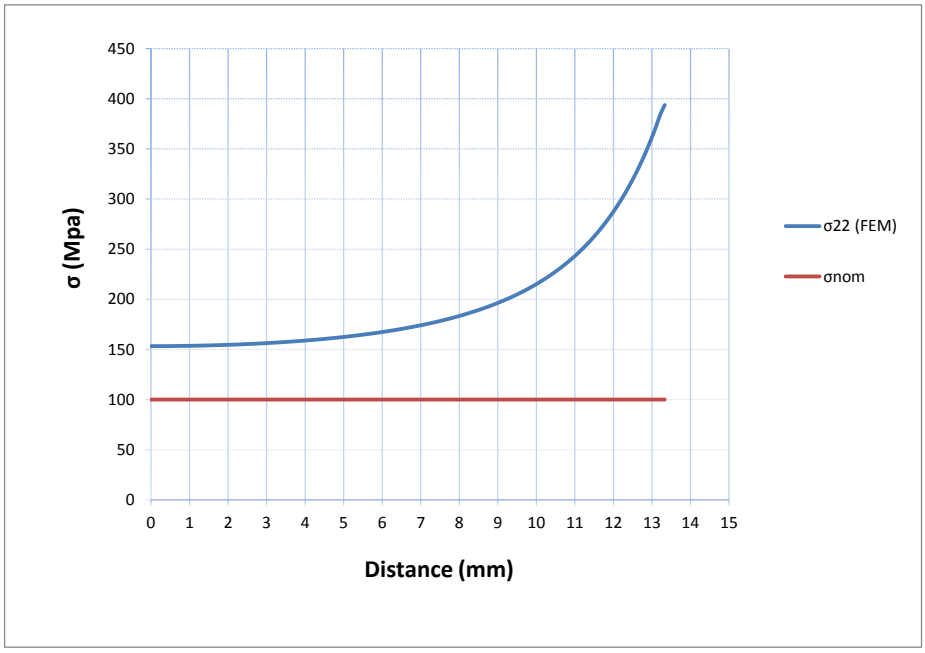

Figure 33 Stress distribution along cross-section with minimum diameter d

From the Figure 33 above it is clear that there is not any kind of stress concentration all over the diameter of the unnotched shaft and its maximum stress value is constant and equal to 100 MPa, whereas the notched shaft appears a stress increase in the outer face.

The stress distribution for the other specimens would be similar to this one, so there is no need for presenting them.

4.2 Graphic Comparison of K_t

The exact calculation of Kt with theoretical values can be supported by Shigley's (Figure 34) and Peterson's (Figure 35) results found in literature and then, can be compared with the numerical results obtained from Abaqus.

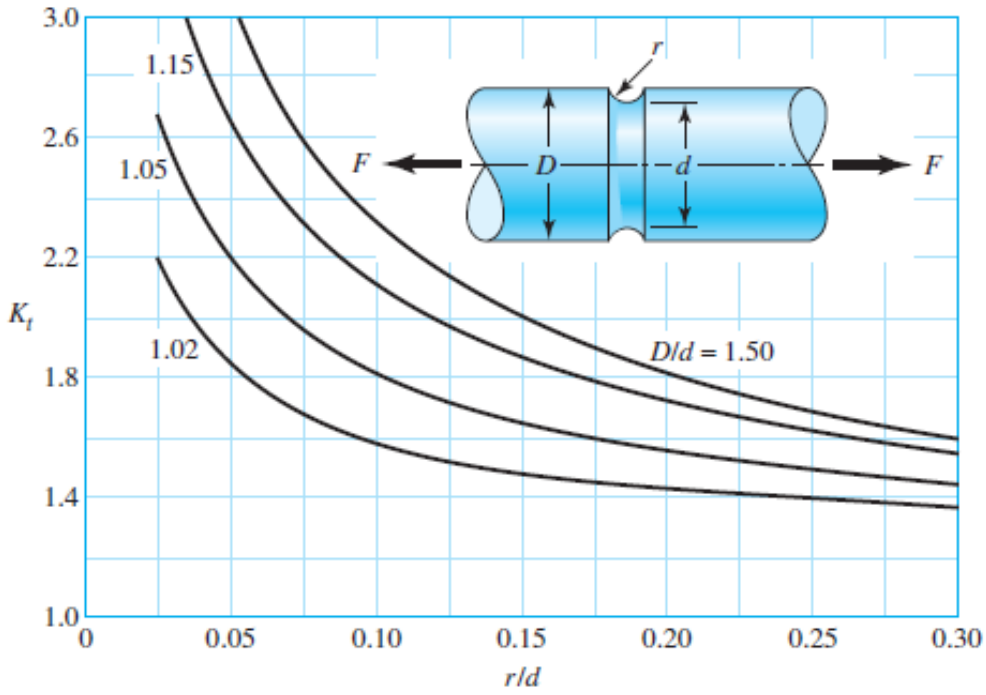

Figure 34 Shigley's chart results for K_t referring to a shaft in tension with a U-shaped groove [5]

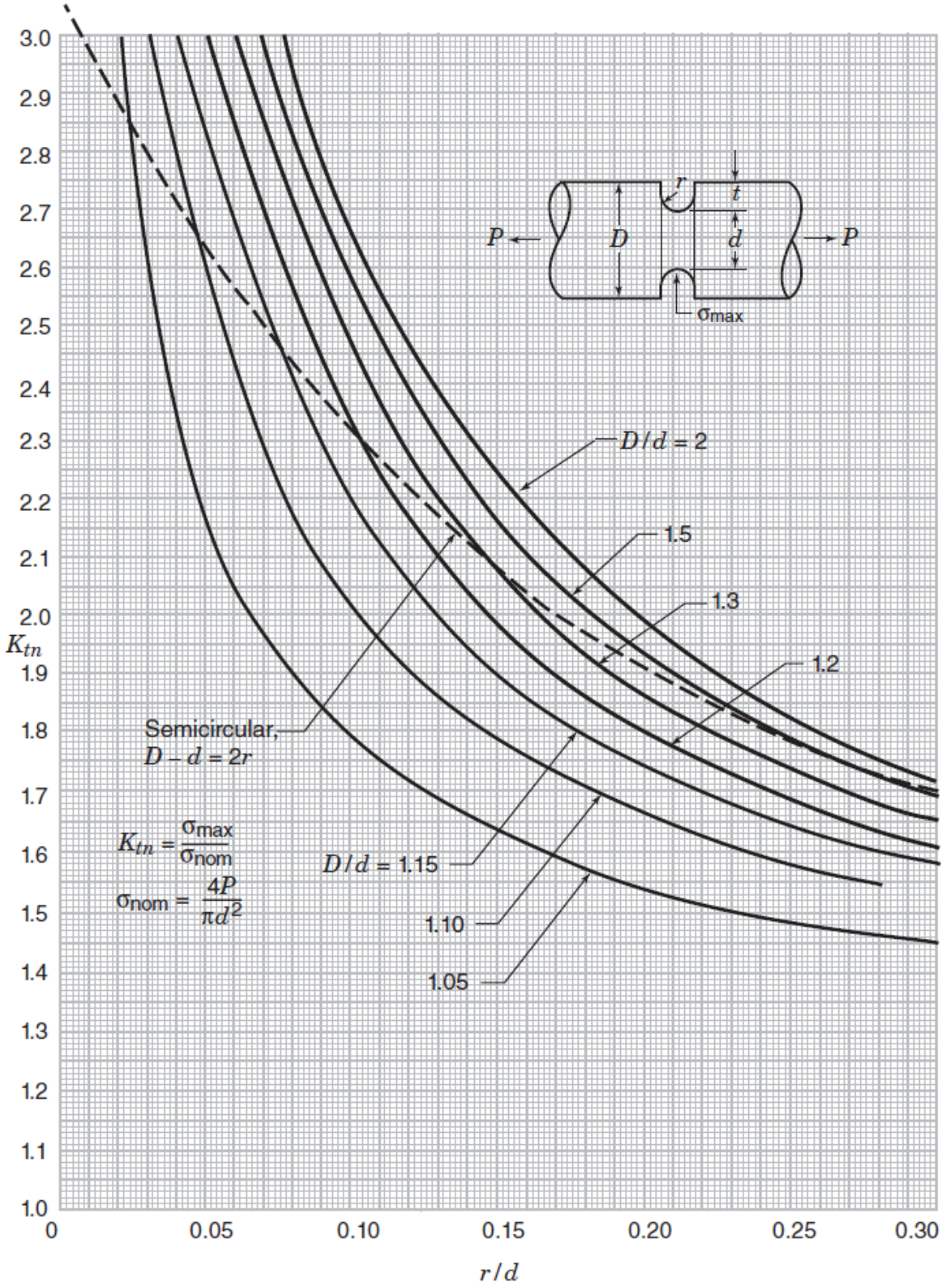

Figure 35 Peterson's stress concentration factors K_t for a shaft in tension with a U-shaped groove [4]

The next figure (Figure 36) shows the graphical comparison between the values of the stress concentration factor as shown in the Peterson's charts above and the ones obtained by the finite elements method.

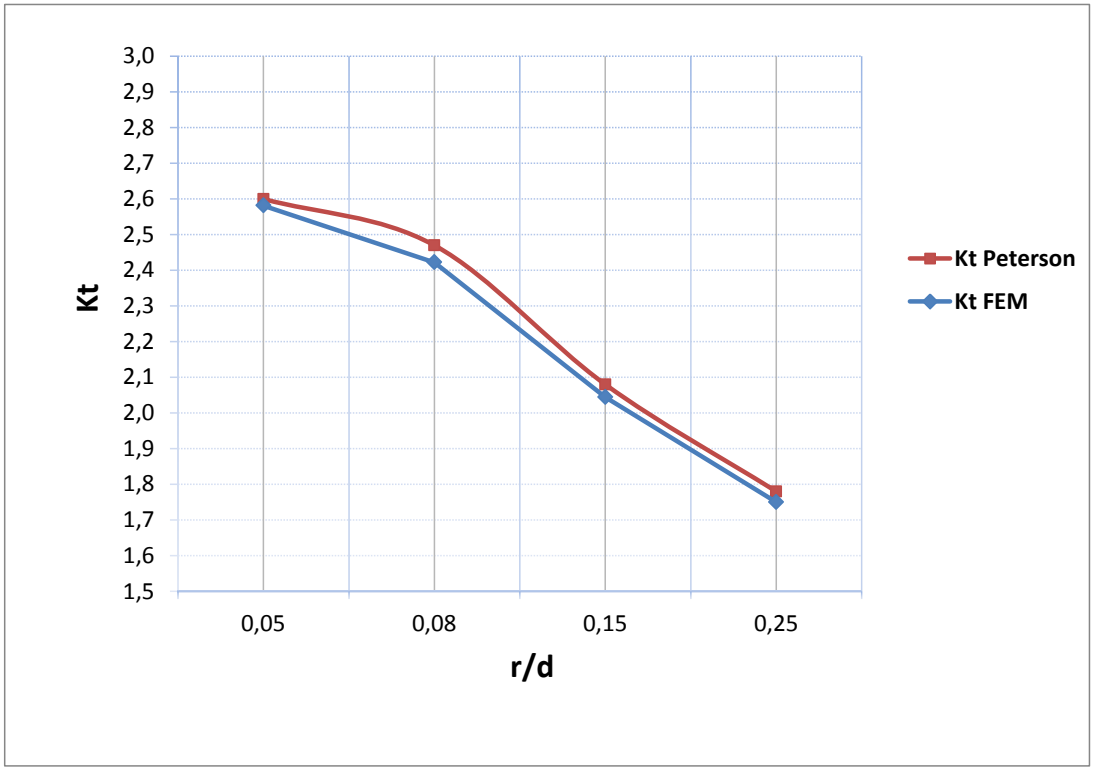

Figure 36 Graphic comparison of K_t values

4.3 Conclusion and comments on results

Most mechanical structures and compartments present various geometrical discontinuities in their shape as well as microstructural discontinuities. Therefore, the determination of the Stress Concentration Factor (K_t) proves to be a major subject for the mechanic engineering industry, serving the purpose of designing safe mechanical structures and obviating structural failures.

Nowadays, the Finite Analysis Method is a useful tool for mechanical engineering that gives the opportunity of analyzing complicated geometries by the help of discretization technique. The effectiveness of this method in calculating quickly and accurately the stress concentration factor K_t is proved by the comparison with values existing in literature. As shown in Table 3, the results obtained from the FEM analysis are quite accurate, with a maximum error of about 1.9 %. The results can be improved even more by improving the mesh and the density of the grid near the area of interest. Those low deviations prove that the Finite Element Method is an accurate way of studying the stress concentration phenomenon and prevent failures, and also can help avoiding errors made from incorrect diagram reading.

However, both theoretical and computational methods of calculating the stress concentration factor are not entirely accurate and can often mislead about the real situation happening in the

critical areas of mechanical structures. Both methods are based on assumptions such as that the material is homogeneous and isotropic, an assumption that is almost never accurate. As a result, engineers and researchers should evaluate in deeper dimensions the characteristics of these problems and study different geometries, dimensions and combination of notches furthermore, in order to overcome any doubtful cases and conclude to more steady results. For example new researches prove that other types of grooves (such as the elliptic ones) can produce reduced stress concentration compared with the semicircular ones [14]. In the last decades, it is safe to claim that the stress concentration analysis is improving with great steps and this will lead to a clearer picture about stress concentration and improving of the mechanical behavior of materials.

REFERENCES

[1] Jack Collins, Henry Busby and George Staab, Mechanical Design of Machine Elements and Machines – A Failure Prevention Perspective, Second Edition, John Wiley and Sons

[2] I. Καρβέλης, Α. Μπαλντούκας, Α. Ντασκαγιάννη, Στοιχεια Μηχανών Σχέδιο, ΟΕΔΒ

[3] Wei-Chih Wang, Photoelasticity, Department of Mechanical Engineering, University of Washington

[4] Walter D. Pilkey, Deborah F. Pilkey and Zhuming Bi, (2020) PETERSON'S STRESS CONCENTRATION FACTORS, Fourth Edition, John Wiley and Sons

[5] Richard G. Budynas and J. Keith Nisbett, SHIGLEY'S MECHANICAL ENGINEERING DESIGN, Tenth Edition

[6] Ν. Αράβας, (2008), Μηχανική των Υλικών – Ανάλυση Ελαστικών Δοκών (Τόμος ΙΙ), Πανεπιστημιακές Εκδόσεις Θεσσαλίας

[7] E.J. Hearn, (1997) PhD in Mechanics of Materials 2 (Third Edition)

[8] Bernard J. Hamrock, Steven R. Schmid and Bo O. Jackobson, (2014) Fundamentals of Machine Elements, Third Edition, Taylor and Francis Group

[9] Jasmin Kisija, Josip Kacmarcik and Aleksandar Karac, (2009) DETERMINATION OF STRESS CONCENTRATION FACTORS VIA NUMERICAL METHODS: BAR OF CIRCULAR CROSS SECTION WITH U-SHAPED GROOVE SUBJECTED TO TENSION AND BENDING, Mechanical Engineering Faculty Zenica

[10] Robert C. Juvinall and Kurt M. Marshek, Fundamentals of Machine – Component Design, Fifth Edition

[11] https://www.enggwave.com/introduction-to-cae-computer-aided-engineering-fea-finite-element-analysis/78184

[12] Pedersen, Niels Leergaard, Aspects of stress in optimal shaft shoulder fillet.

[13] Abaqus Analysis User's Guide (6.14)

[14] R.U. Ahsan, P. Prachurja, A.R.M. Ali and M.A.H. Mamun, (2013) DETERMINATION OF EFFECT OF ELLIPTIC NOTCHES AND GROOVES ON STRESS CONCENTRATION FACTORS ON NOTCHED BAR IN TENSION AND GROOVED SHAFT UNDER TORSION, Department of Mechanical Engineering, Bangladesh University of Engineering and Technology

APPENDIX

The input files from specimen 3005 created by Abaqus environment. Only a portion of the input file is presented here in order to save space and reduce the size of the text.

```
*Heading
** Job name: Job-1 Model name: Model-1
** Generated by: Abaqus/CAE 2016.HF2
*Preprint, echo=NO, model=NO, history=NO, contact=NO
**
** PARTS
**
*Part, name=Part-1
*Node
      1,          20.,          70.
      2,           0.,          70.
      3,           0.,           0.
      4,          20.,           0.
      5,          20.,          76.
      6,   10.1005049,    80.100502
      7,           6.,          90.
      8,           0.,          90.
      9,          20.,          83.
     10,          13.,          90.
     11,          20.,   88.1999969
     12,   18.2000008,          90.
     13,   19.2632694,          70.
     14,   18.5121765,          70.
     15,   17.7464409,          70.
     16,   16.9657784,          70.
     17,   16.1698933,          70.
     18,   15.3584948,          70.
     19,   14.5312767,          70.
     20,   13.6879311,          70.
     21,   12.8281441,          70.
     22,   11.9515963,          70.
     23,   11.0579586,          70.
     24,   10.1468992,          70.
     25,   9.21807861,          70.
   5930,   18.4591484,   88.9301682
   5931,   18.4983158,   88.8758545
   5932,   18.5393944,   88.8229675
   5933,   18.5823364,   88.7715912
   5934,   18.6270847,   88.7217712
   5935,   18.6735821,    88.673584
   5936,   18.7217712,   88.6270828
   5937,   18.7715874,   88.5823364
   5938,   18.8229694,   88.5393982
   5939,   18.8758526,   88.4983139
   5940,   18.9301682,   88.4591522
   5941,   18.9858456,   88.4219437
   5942,   19.0428162,   88.3867569
   5943,   19.1010075,   88.3536148
   5944,   19.1603432,   88.3225784
   5945,   19.2207489,   88.2936783
   5946,   19.2821484,   88.2669525
   5947,   19.3444614,   88.2424316
   5948,   19.4076118,   88.2201538
   5949,   19.4715157,   88.2001495
   5950,   19.5360928,   88.1824341
   5951,    19.601263,   88.1670303
   5952,   19.6669388,   88.1539688
   5953,   19.7330399,   88.1432571
   5954,   19.7994823,   88.1349106
   5955,   19.8661785,   88.1289444
   5956,   19.9330463,   88.1253586
```

```
*Element, type=CAX4
     1,     1,    13,   550,   206
     2,    13,    14,   551,   550
     3,    14,    15,   552,   551
     4,    15,    16,   553,   552
     5,    16,    17,   554,   553
     6,    17,    18,   555,   554
     7,    18,    19,   556,   555
     8,    19,    20,   557,   556
     9,    20,    21,   558,   557
    10,    21,    22,   559,   558
    11,    22,    23,   560,   559
    12,    23,    24,   561,   560
    13,    24,    25,   562,   561
    14,    25,    26,   563,   562
    15,    26,    27,   564,   563
    16,    27,    28,   565,   564
    17,    28,    29,   566,   565
    18,    29,    30,   567,   566
    19,    30,    31,   568,   567
    20,    31,    32,   569,   568
    21,    32,    33,   570,   569
    22,    33,     2,    34,   570
    23,   206,   550,   571,   205
    24,   550,   551,   572,   571
    25,   551,   552,   573,   572
    26,   552,   553,   574,   573
    27,   553,   554,   575,   574
    28,   554,   555,   576,   575
    29,   555,   556,   577,   576
    30,   556,   557,   578,   577
```

```
5715, 5929, 5930,  489,  490
5716, 5930, 5931,  488,  489
5717, 5931, 5932,  487,  488
5718, 5932, 5933,  486,  487
5719, 5933, 5934,  485,  486
5720, 5934, 5935,  484,  485
5721, 5935, 5936,  483,  484
5722, 5936, 5937,  482,  483
5723, 5937, 5938,  481,  482
5724, 5938, 5939,  480,  481
5725, 5939, 5940,  479,  480
5726, 5940, 5941,  478,  479
5727, 5941, 5942,  477,  478
5728, 5942, 5943,  476,  477
5729, 5943, 5944,  475,  476
5730, 5944, 5945,  474,  475
5731, 5945, 5946,  473,  474
5732, 5946, 5947,  472,  473
5733, 5947, 5948,  471,  472
5734, 5948, 5949,  470,  471
5735, 5949, 5950,  469,  470
5736, 5950, 5951,  468,  469
5737, 5951, 5952,  467,  468
5738, 5952, 5953,  466,  467
5739, 5953, 5954,  465,  466
5740, 5954, 5955,  464,  465
5741, 5955, 5956,  463,  464
5742, 5956,  462,   11,  463
```

The nodes range between (1 – 5956) and the elements range between (1 – 5742).

```
*Nset, nset=Set-1, generate
    1,  5956,     1
*Elset, elset=Set-1, generate
    1,  5742,     1
** Section: Section-1
*Solid Section, elset=Set-1, material=Material-1
,
*End Part
**
**
** ASSEMBLY
**
*Assembly, name=Assembly
**
*Instance, name=Part-1-1, part=Part-1
*End Instance
**
*Nset, nset=Set-1, instance=Part-1-1
   2,   3,   8,  34,  35,  36,  37,  38,  39,  40,  41,  42,  43,  44,  45,  46
  47,  48,  49,  50,  51,  52,  53,  54,  55,  56,  57,  58,  59,  60,  61,  62
  63,  64,  65,  66,  67,  68,  69,  70,  71,  72,  73,  74,  75,  76,  77,  78
  79,  80,  81,  82,  83,  84,  85,  86,  87,  88,  89,  90,  91,  92,  93,  94
  95,  96,  97,  98,  99, 100, 101, 102, 103, 104, 105, 106, 107, 108, 109, 297
 298, 299, 300, 301, 302, 303, 304, 305, 306, 307, 308, 309, 310, 311, 312, 313
 314, 315, 316, 317
```

```
*Elset, elset=Set-1, instance=Part-1-1
   22,   44,   66,   88,  110,  132,  154,  176,  198,  220,  242,  264,  286,  308,  330,  352
  374,  396,  418,  440,  462,  484,  506,  528,  550,  572,  594,  616,  638,  660,  682,  704
  726,  748,  770,  792,  814,  836,  858,  880,  902,  924,  946,  968,  990, 1012, 1034, 1056
 1078, 1100, 1122, 1144, 1166, 1188, 1210, 1232, 1254, 1276, 1298, 1320, 1342, 1364, 1386, 1408
 1430, 1452, 1474, 1496, 1518, 1540, 1562, 1584, 1606, 1628, 1650, 1672, 1694, 2421, 2422, 2423
 2424, 2425, 2426, 2427, 2428, 2429, 2430, 2431, 2432, 2433, 2434, 2435, 2436, 2437, 2438, 2439
 2440, 2441, 2442
*Nset, nset=Set-2, instance=Part-1-1
   7,   8,  10,  12, 281, 282, 283, 284, 285, 286, 287, 288, 289, 290, 291, 292
 293, 294, 295, 296, 361, 362, 363, 364, 365, 366, 367, 368, 369, 370, 371, 372
 373, 374, 375, 376, 377, 378, 379, 380, 381, 382, 383, 384, 385, 386, 387, 388
 389, 506, 507, 508, 509, 510, 511, 512, 513, 514, 515, 516, 517, 518, 519, 520
 521, 522, 523, 524, 525, 526, 527, 528, 529, 530, 531, 532, 533, 534, 535, 536
 537, 538, 539, 540, 541, 542, 543, 544, 545, 546, 547, 548, 549
*Elset, elset=Set-2, instance=Part-1-1
 2090, 2112, 2134, 2156, 2178, 2200, 2222, 2244, 2266, 2288, 2310, 2332, 2354, 2376, 2398, 2420
 2442, 2486, 2530, 2574, 2618, 2662, 2706, 2750, 2794, 2838, 2882, 2926, 2970, 3014, 3058, 3102
 3146, 3190, 3234, 3278, 3322, 3366, 3410, 3454, 3498, 3542, 3586, 3630, 3674, 3718, 3762, 3763
 3807, 3851, 3895, 3939, 3983, 4027, 4071, 4115, 4159, 4203, 4247, 4291, 4335, 4379, 4423, 4467
 4511, 4555, 4599, 4643, 4687, 4731, 4775, 4819, 4863, 4907, 4951, 4995, 5039, 5083, 5127, 5171
 5215, 5259, 5303, 5347, 5391, 5435, 5479, 5523, 5567, 5611, 5655, 5699
*Elset, elset=_Surf-1_S3, internal, instance=Part-1-1, generate
 1673,  1694,     1
*Surface, type=ELEMENT, name=Surf-1
_Surf-1_S3, S3
*End Assembly
**
** MATERIALS
**
*Material, name=Material-1
*Elastic
210000., 0.33
** BOUNDARY CONDITIONS
**
** Name: BC-1 Type: Symmetry/Antisymmetry/Encastre
*Boundary
Set-1, XSYMM
** Name: BC-2 Type: Displacement/Rotation
*Boundary
Set-2, 2, 2
Set-2, 6, 6
** ----------------------------------------------------------------
**
** STEP: Step-1
**
*Step, name=Step-1, nlgeom=NO
*Static
1., 1., 1e-05, 1.
**
** LOADS
**
** Name: Load-1   Type: Pressure
*Dsload
Surf-1, P, -100.
**
** OUTPUT REQUESTS
**
*Restart, write, frequency=0
**
** FIELD OUTPUT: F-Output-1
**
*Output, field, variable=PRESELECT
**
** HISTORY OUTPUT: H-Output-1
**
*Output, history, variable=PRESELECT
*End Step
```